

Effect of Titania Phase Composition in  $\text{WO}_3/\text{TiO}_2$  Catalysts on Catalytic Properties in  
Dehydration of Ethanol to Diethyl Ether

Miss Phatthraporn Termvoratham



A Thesis Submitted in Partial Fulfillment of the Requirements  
for the Degree of Master of Engineering in Chemical Engineering

Department of Chemical Engineering

Faculty of Engineering

Chulalongkorn University

Academic Year 2019

Copyright of Chulalongkorn University

ผลขององค์ประกอบไทเทเนียมเฟสในตัวเร่งปฏิกิริยา  $WO_3/TiO_2$  ต่อสมบัติการเร่งปฏิกิริยาดีไฮเดรชัน  
ของเอทานอลเป็นไดเอทิลอีเทอร์



วิทยานิพนธ์นี้เป็นส่วนหนึ่งของการศึกษาตามหลักสูตรปริญญาวิศวกรรมศาสตรมหาบัณฑิต  
สาขาวิชาวิศวกรรมเคมี ภาควิชาวิศวกรรมเคมี  
คณะวิศวกรรมศาสตร์ จุฬาลงกรณ์มหาวิทยาลัย  
ปีการศึกษา 2562  
ลิขสิทธิ์ของจุฬาลงกรณ์มหาวิทยาลัย

Thesis Title                      Effect of Titania Phase Composition in WO<sub>3</sub>/TiO<sub>2</sub>  
Catalysts on Catalytic Properties in Dehydration of  
Ethanol to Diethyl Ether  
By                                      Miss Phatthraporn Termvoratham  
Field of Study                      Chemical Engineering  
Thesis Advisor                      Professor Dr. BUNJERD JONGSOMJIT

---

Accepted by the Faculty of Engineering, Chulalongkorn University in Partial  
Fulfillment of the Requirement for the Master of Engineering

..... Dean of the Faculty of Engineering  
(Professor Dr. SUPOT TEACHAVORASINSKUN)

THESIS COMMITTEE

..... Chairman  
(Assistant Professor Dr. NATTAPORN TONANON)

..... Thesis Advisor  
(Professor Dr. BUNJERD JONGSOMJIT)

..... Examiner  
(Associate Professor Dr. ANONGNAT  
SOMWANGTHANAROJ)

..... External Examiner  
(Assistant Professor Dr. Sasiradee Jantasee)

ภัทรภรณ์ เต็มวรรธธรรม : ผลขององค์ประกอบไททาเนียเฟสในตัวเร่งปฏิกิริยา  
 $WO_3/TiO_2$  ต่อสมบัติการเร่งปฏิกิริยาดีไฮเดรชันของเอทานอลเป็นไดเอทิลอีเทอร์. (Effect of Titania Phase Composition in  $WO_3/TiO_2$  Catalysts on Catalytic Properties in Dehydration of Ethanol to Diethyl Ether) อ.ที่ปรึกษาหลัก : ศ.ดร.บรรเจิด จงสมจิตร

ในปัจจุบันผลิตภัณฑ์ทางการเกษตรหลายชนิดสามารถนำไปใช้เป็นวัตถุดิบในการผลิตไบโอเอทานอลและเปลี่ยนเป็นสารที่มีคุณค่าเช่นเอทิลีนและไดเอทิลอีเทอร์ สิ่งนี้สามารถเกิดขึ้นได้ผ่านตัวเร่งปฏิกิริยา  $WO_3/TiO_2$  ซึ่งเฟสอะนาเทสของไททาเนียมักจะมีควมว่องไวที่ดีกว่าเฟสรูไทล์ต่อดีไฮเดรชันของเอทานอลเป็นไดเอทิลอีเทอร์และเอทิลีน อย่างไรก็ตามเฟสอะนาเทสบริสุทธิ์ของไททาเนียอาจไม่ให้คุณสมบัติการเร่งปฏิกิริยาที่ดีที่สุด ดังนั้นงานวิจัยนี้จึงศึกษาผลกระทบของตัวเร่งปฏิกิริยาทั้งสแตนด์บายรองรับไททาเนียที่มีองค์ประกอบเฟสที่แตกต่างกันของไททาเนียซึ่งประกอบด้วยเฟสอะนาเทสและรูไทล์ที่มีสัดส่วนต่าง ๆ ( $TiO_2$ -R0,  $TiO_2$ -R25,  $TiO_2$ -R75,  $TiO_2$ -R75 และ  $TiO_2$ -R100) ตัวเร่งปฏิกิริยาถูกพิจารณาคุณสมบัติทางกายภาพและวิเคราะห์คุณสมบัติของตัวเร่งปฏิกิริยาแบบไดนามิก พบว่าตัวเร่งปฏิกิริยา  $WO_3/TiO_2$ -R50 ให้เอทิลีนสูงสุด (ผลผลิต 79.6%) ที่ 350 °C และไดเอทิลอีเทอร์ (ผลผลิต 9.0%) ที่ 300 °C เนื่องจากมีอัตราส่วนกรดอ่อนต่อกรดแก่สูงสุด ดังนั้นตัวเร่งปฏิกิริยา  $WO_3/TiO_2$ -R50 จึงถูกเลือกเพื่อศึกษาความเสถียรของตัวเร่งปฏิกิริยาต่อการเร่งปฏิกิริยาดีไฮเดรชันของเอทานอล พบว่าตัวเร่งปฏิกิริยาเสถียรต่อการเร่งปฏิกิริยาดีไฮเดรชันของเอทานอลภายใน 2 ชั่วโมง แต่ไม่เสถียรต่อไดเอทิลอีเทอร์ โดยระยะเวลาการทำปฏิกิริยานานส่งผลต่อการเกิดโค้กซึ่งเป็นปัจจัยที่ลดตำแหน่งที่ว่องไวบนพื้นที่ผิวนำไปสู่การเร่งปฏิกิริยาที่ลดลง

สาขาวิชา วิศวกรรมเคมี  
 ปีการศึกษา 2562

ลายมือชื่อนิสิต .....  
 ลายมือชื่อ อ.ที่ปรึกษาหลัก .....

# # 6170950421 : MAJOR CHEMICAL ENGINEERING

KEYWORD:

Phatthraporn Termvoratham : Effect of Titania Phase Composition in  $WO_3/TiO_2$  Catalysts on Catalytic Properties in Dehydration of Ethanol to Diethyl Ether. Advisor: Prof. Dr. BUNJERD JONGSOMJIT

At the present, several agricultural products can be used as raw materials for bio-ethanol production and consequently converted it into many valuable substances such as ethylene and diethyl ether. This can undergo via  $WO_3/TiO_2$  catalyst in which the anatase phase of titania usually has a better activity on ethanol dehydration to diethyl ether and ethylene than rutile phase. However, pure anatase phase of titania perhaps does not give the best of catalytic properties. So, this study investigates on the effects of tungsten on titania-supported catalysts with different phase composition of titania consisting of anatase and rutile phase with various proportion ( $TiO_2$ -R0,  $TiO_2$ -R25,  $TiO_2$ -R50,  $TiO_2$ -R75 and  $TiO_2$ -R100). The catalysts were characterized to determine physical properties and analyzed dynamic catalytic properties. It was found that the  $WO_3/TiO_2$ -R50 catalyst gave the highest ethylene (79.6% yield) at 350°C and DEE (9.0% yield) at 300 °C due to it contained the highest weak to strong acid site ratio. Thus,  $WO_3/TiO_2$ -R50 catalyst was selected to study the stability of the catalysts on ethanol dehydration reaction. It was found that the catalyst was stable to the ethanol dehydration reaction to ethylene within 2 hours, but is not stable to diethyl ether by long ethanol dehydration reaction time effects coke formation. It is a factor to decrease active site on surface area leading to lower catalytic activity.

Field of Study: Chemical Engineering

Student's Signature .....

Academic Year: 2019

Advisor's Signature .....

## ACKNOWLEDGEMENTS

The author would like to express the deepest gratitude to her thesis advisor, Professor Bunjerd Jongsomjit for his guidance and support for all solving problems throughout this research. In addition, the author is appreciative of patience and motivation with good wishes for her to be successful. This thesis cannot be achieved without him.

Moreover, the author would like to thank chairman of the committee, Asst. Prof. Dr. Nattaporn Tonanon, and members of the thesis committee, Assoc. Prof. Dr. Anongnat Somwangthanaroj and Asst. Prof. Dr. Sasiradee Jantasee for their suggestions and revision of this thesis.

The author would like to thank for the Grant for International Research Integration: Chula Research Scholar, Ratchadaphiseksomphot Endowment Fund and Grant for Research: Government Budget, Chulalongkorn University (2018) for financial support of this research also.

Most importantly, the author appreciates her family who were always encouraged with love, understanding and supported. The author would like to express his deep gratitude to her friends at Center of Excellence on Catalysis and Catalytic Reaction Engineering and others for their help throughout this research.

จุฬาลงกรณ์มหาวิทยาลัย  
CHULALONGKORN UNIVERSITY

Phatthraporn Termvoratham

## TABLE OF CONTENTS

	Page
.....	iii
ABSTRACT (THAI).....	iii
.....	iv
ABSTRACT (ENGLISH).....	iv
ACKNOWLEDGEMENTS.....	v
TABLE OF CONTENTS.....	vi
LIST OF TABLES.....	ix
LIST OF FIGURES.....	x
CHAPTER 1 INTRODUCTION.....	1
1.1 Introduction.....	1
1.2 Motivation.....	4
1.3 Research objectives.....	5
1.4 Research scopes.....	5
1.5 Expected benefits.....	5
CHAPTER 2 THEORY AND LITERATURE REVIEWS.....	6
2.1 Ethanol.....	6
2.2 Ethanol dehydration.....	6
2.3 Catalysts.....	7
2.4 Titanium (IV) oxide (TiO <sub>2</sub> ).....	8
2.5 Incipient wetness impregnation.....	8
2.6 Literature reviews.....	9

CHAPTER 3 EXPERIMENTS .....	12
3.1 Research methodology .....	12
3.2 Catalyst preparation .....	13
3.3 Catalyst characterization.....	14
3.4 Reaction study of ethanol dehydration .....	15
3.5 Reaction test .....	16
3.6 Analysis and Calculation.....	16
3.7 Research plan .....	17
CHAPTER 4 RESULTS AND DISCUSSION .....	18
Part I: The characteristic and catalytic activity of $WO_3/TiO_2$ catalysts with different phases of $TiO_2$ (R0, R25, R50, R75 and R100).....	19
4.1.2 Scanning electron microscope (SEM) and energy dispersive X-ray spectroscopy (EDX) .....	20
4.1.3 $N_2$ physisorption .....	28
4.1.4 Ammonia temperature-programmed desorption ( $NH_3$ -TPD).....	30
4.1.5 Reaction test.....	31
4.1.6 Dispersive X-ray spectroscopy (EDX) for spent catalysts.....	36
4.1.7 Catalysts appearance .....	37
4.1.8 X-ray diffraction (XRD) for spent catalysts .....	37
Part II: Stability of $WO_3/TiO_2$ catalyst having the highest catalytic activity (from Part I).....	39
4.2.1 Reaction test.....	39
4.2.2 X-ray diffraction (XRD) for spent catalysts .....	43
4.2.3 Scanning electron microscope (SEM) and energy Dispersive X-ray spectroscopy (EDX) for spent catalysts.....	44



4.2.4 Catalysts appearance .....	50
Part III: The comparison of catalysts for diethyl ether and ethylene synthesis and their catalytic activity .....	51
CHAPTER 5 CONCLUSIONS AND RECOMMENDATIONS .....	52
5.1 Conclusions .....	52
5.2 Recommendations .....	53
REFERENCES .....	54
APPENDIX.....	57
APPENDIX A CALCULATION FOR CATALYST PREPARATION .....	58
APPENDIX B CALCULATION FOR ACIDITY .....	60
APPENDIX C CALIBRATION CURVES OF REACTANT AND PRODUCTS.....	61
APPENDIX D CHROMATOGRAM.....	64
APPENDIX E CALCULATION FOR CRYSTALLITE SIZE (SCHERRER EQUATION).....	65
APPENDIX F LIST OF PUBLICATION.....	66
VITA.....	67

## LIST OF TABLES

	Page
Table 1 Schedule of the research plan.....	17
Table 2 The amount of elemental distribution on the catalyst surface.....	23
Table 3 The average width of particle sizes of all catalysts.....	24
Table 4 The average length of particle sizes of all catalysts.....	24
Table 5 Textural properties of all catalysts with different phases of TiO <sub>2</sub> .....	28
Table 6 The amount of acidity of all catalysts with different phases of TiO <sub>2</sub> .....	31
Table 7 Ethanol conversion, product selectivity and product yield.....	35
Table 8 The amount of %carbon in the spent catalysts.....	36
Table 9 Ethanol conversion, product selectivity and product yield for the ethanol dehydration reaction at 300 °C.....	40
Table 10 Ethanol conversion, product selectivity and product yield for the ethanol dehydration reaction at 350 °C.....	42
Table 11 Average crystal size of the WO <sub>3</sub> /TiO <sub>2</sub> -R50 catalysts.....	43
Table 12 The average width of particle sizes of WO <sub>3</sub> /TiO <sub>2</sub> -R50 catalysts.....	48
Table 13 The average length of particle sizes of WO <sub>3</sub> /TiO <sub>2</sub> -R50 catalysts.....	48
Table 14 The amount of %carbon in the spent catalysts with operating temperature.....	49
Table 15 Comparison of catalysts for DEE and ethylene synthesis and their catalytic activity.....	51

## LIST OF FIGURES

	Page
Figure 1 shows the global production and consumption of ethanol from 2010 - 2016, averaging 3.5% per year [1] .....	1
Figure 2 shows the production and consumption of ethanol of each country [1].....	2
Figure 3 Statistic report of diethyl ether imports [9] .....	3
Figure 4 Diagram for bioethanol production from natural sources [16] .....	6
Figure 5 Schematic of wet impregnation and incipient wetness impregnation techniques.....	9
Figure 6 Experimental set up for reaction test .....	15
Figure 7 XRD patterns of catalysts with different phase of TiO <sub>2</sub> .....	19
Figure 8 SEM micrographs of all catalysts with different phase compositions of TiO <sub>2</sub> .....	20
Figure 9 EDX mapping of WO <sub>3</sub> /TiO <sub>2</sub> -R0 .....	21
Figure 10 EDX mapping of WO <sub>3</sub> /TiO <sub>2</sub> -R25.....	21
Figure 11 EDX mapping of WO <sub>3</sub> /TiO <sub>2</sub> -R50.....	22
Figure 12 EDX mapping of WO <sub>3</sub> /TiO <sub>2</sub> -R75.....	22
Figure 13 EDX mapping of WO <sub>3</sub> /TiO <sub>2</sub> -R100.....	23
Figure 14 Histogram graph on width of particle sizes of all catalysts .....	25
Figure 15 Histogram graph on length of particle sizes of all catalysts.....	26
Figure 16 The average width particle size of all catalysts.....	27
Figure 17 The average length particle size of all catalysts.....	27
Figure 18 N <sub>2</sub> adsorption-desorption isotherms of WO <sub>3</sub> /TiO <sub>2</sub> -R0, WO <sub>3</sub> /TiO <sub>2</sub> -R50 and WO <sub>3</sub> /TiO <sub>2</sub> -R100 catalysts .....	29

Figure 19 The pore size distribution of $\text{WO}_3/\text{TiO}_2\text{-R0}$ , $\text{WO}_3/\text{TiO}_2\text{-R50}$ and $\text{WO}_3/\text{TiO}_2\text{-R100}$ catalysts.....	29
Figure 20 $\text{NH}_3\text{-TPD}$ profiles of all catalysts with different phases of $\text{TiO}_2$ .....	30
Figure 21 Ethanol Conversion of all catalysts with different phase of $\text{TiO}_2$ .....	32
Figure 22 Product selectivity of all catalysts with different phase of $\text{TiO}_2$ .....	33
Figure 23 Product yields of all catalysts with different phase of $\text{TiO}_2$ .....	34
Figure 24 The appearance of fresh catalysts with different phase of $\text{TiO}_2$ .....	37
Figure 25 The appearance of spent catalysts with different phase of $\text{TiO}_2$ .....	37
Figure 26 XRD patterns of the spent catalysts with different phase of $\text{TiO}_2$ .....	38
Figure 27 Activities on the ethanol dehydration at 300 °C .....	39
Figure 28 Activities on the ethanol dehydration at 350 °C .....	41
Figure 29 XRD patterns of the spent $\text{WO}_3/\text{TiO}_2\text{-R50}$ catalysts .....	44
Figure 30 SEM micrographs of $\text{WO}_3/\text{TiO}_2\text{-R50}$ catalysts.....	45
Figure 31 Histogram graph on width of particle sizes of all catalysts.....	46
Figure 32 Histogram graph on length of particle sizes of all catalysts.....	47
Figure 33 The average width particle size of all catalysts.....	48
Figure 34 The average length particle size of all catalysts.....	49
Figure 35 The appearance of $\text{WO}_3/\text{TiO}_2\text{-R50}$ catalyst (a) fresh catalysts (b) spent catalysts for ethanol dehydration at 300 °C (c) spent catalysts for ethanol dehydration at 350 °C .....	50

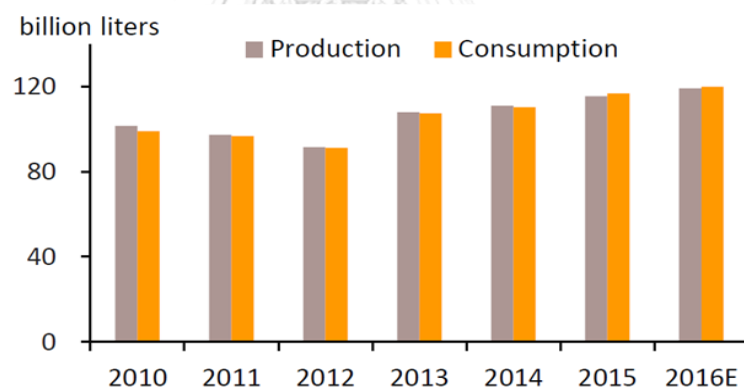
# CHAPTER 1

## INTRODUCTION

### 1.1 Introduction

At present, many agencies concern on environmental issues arising from fossil fuel usage. As well as the limited amount of fossil fuel source, many industries see the importance of improving production processes in line with global trends by studying on renewable and clean energy. In addition, due to the problems of agricultural products that have exceeded the demand for consumption, the government in many countries (such as Brazil and Thailand) tries to find the solutions to solve problems by increasing the value of these products more. For instance, the government has a policy to use agricultural products as a raw material replaced on fossil fuel.

**World Ethanol Production and Consumption**



Source: OECD-FAO

**Figure 1** shows the global production and consumption of ethanol from 2010 - 2016, averaging 3.5% per year [1]

**Global Ethanol Consumption and Production by Volume (2016)**

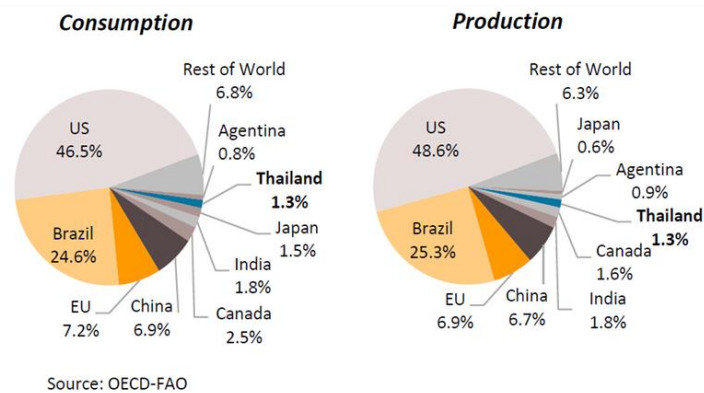


**Figure 2** shows the production and consumption of ethanol of each country [1]

At present, Thailand has produced ethanol to be blended with gasoline called "gasohol" because the government has a policy to support the use of biofuels to replace fossil fuels such as the government to use money from the fuel fund for subsidy of gasohol E20 and gasohol E85 (20% and 85% ethanol mixtures, respectively) [2]. Several agricultural products such as sugarcane, starch, molasses, cassava, corn, lignocelluloses etc. can be used as raw materials for the production of bio-ethanol. The production process depends on raw materials used and fermentation process [3-5] is usually applied. However, many countries such as Brazil and Thailand mostly use ethanol to blend with gasoline with highly ratio to be used as fuel for vehicles that causes of corrosion in engine. [6] Because ethanol blends with gasoline affect different engines in each model. There are 2 main issues: 1) Ethanol is a substance that has good moisture absorption properties. In the production, must avoid having to mix water because the amount of water that is mixed affects the poor mix of gasoline, causing it to not be able to use this fuel. 2) Fuel compatibility, especially with older cars found that corrosion and other damage in the fuel system cause damage to the engine [7].

However, Thailand Integrated Energy Blueprint or TIEB 2015 is under the Energy Efficiency Plan (EEP 2015) targets 1.2 million electric plug-in hybrid and electric vehicle batteries (BEV) by 2036. One of the policies to drive the plan such as electric vehicles (EV) that are promoted by the BOI, will receive excise tax reduction from 2% to 0% since 1 January 2020 until 31 December 2022, totaling 3 years to promote vehicle that are environmentally friendly faster [8].

In addition to ethanol blending in gasoline, ethanol is a substance that has economic value and can be converted into many valuable substances such as diethyl ether, ethylene, etc. Diethyl ether that is used in Thailand only from imports. In 2018, Thailand imported Diethyl ether 62.205 tons with a total value of over 12 million baht as shows in **Figure 3** [9]. The production process mainly uses sulfuric acid as a catalyst, therefore it is necessary to separate the sulfuric acid from the product, which is a complicated procedure [4]. Diethyl ether is used as solvent in chemical laboratories and pharmaceutical industries, used as extract for fat, oil, wax and resin, used in plastic production and used as an anesthetic in medical [3, 10].

HS-CODE	29	ORGANIC CHEMICAL
	2909	Ethers, ether-alcohols, ether-phenols, ether-alcohol-phenols, alcohol peroxides, ether peroxides, ketone peroxides (whether or not chemically defined), and their halogenated, sulphonated, nitrated or nitrosated derivatives.
	29091100	Diethyl ether
	Statistic code : 000	Diethyl ether (KGM)

COUNTRY		Dec 2018		Jan - Dec 2018	
		Quantity	CIF (Baht)	Quantity	CIF (Baht)
BE	BELGIUM	0	0	170	62,241
DE	GERMANY	0	0	27,815	7,865,341
IN	INDIA	511	102,092	27,731	2,260,861
JP	JAPAN	12	10,007	94	99,917
KR	KOREA,REPUBLIC OF	0	0	1,142	291,495
ES	SPAIN	0	0	2,887	1,153,935
GB	UNITED KINGDOM	0	0	35	16,627
US	UNITED STATES	0	0	2,331	728,804
SUM		523	112,099	62,205	12,479,221

**Figure 3** Statistic report of diethyl ether imports [9]

Reactions that use ethanol as a raw material can produce the products by many reactions. The main reactions that occur are 3 reaction as follows; [11, 12]

Dehydration (Endothermic reaction)



Dehydration (Exothermic reaction)



Dehydrogenation (Endothermic reaction)



Many researchers studied on the catalytic dehydration of ethanol by using alumina, MgO, alumina-silica and  $\text{WO}_3/\text{TiO}_2$  catalyst [10, 13, 14]. As known, the anatase phase of titania has a better effect on dehydration of ethanol to diethyl ether than rutile phase in dynamic catalytic properties such as activity, selectivity and stability. However, pure anatase phase of titania does not give the best of catalytic properties. Therefore, this study is interesting to find the optimal portion in the anatase to rutile phase of titania that is suitable for dynamics catalytic properties [15].

Therefore, this study shows the effects of tungsten on titania supported catalysts with different titania phases consisting of anatase and rutile phase with various portion. Then, the  $\text{WO}_3/\text{TiO}_2$  catalysts were prepared by incipient wetness impregnation. The effect of different catalysts on dehydration of ethanol to diethyl ether and ethylene was investigated. The characteristics of catalyst were analyzed by X-ray diffraction (XRD), scanning electron microscope (SEM) and electron dispersive X-ray (EDX) spectroscopy,  $\text{N}_2$ -physisorption, temperature-programmed desorption of ammonia ( $\text{NH}_3$ -TPD) techniques and measured the catalytic properties by ethanol dehydration under atmospheric pressure and temperature interval range of 200 – 400 °C. Furthermore, the catalyst with the highest dynamic catalytic properties was tested for stability by reaction test with time on stream and investigated the deactivation causes.

## 1.2 Motivation

Effects of anatase and rutile phase of titania in  $\text{WO}_3/\text{TiO}_2$  catalysts on catalytic dehydration of ethanol to diethyl ether are interesting. Although anatase phase has a better effect on the dehydration of ethanol than rutile phase, the mixture of titania phase result in higher diethyl ether yield. So, this study aims to study different phase composition of titania that is appropriate for catalytic ethanol dehydration to diethyl ether.



### 1.3 Research objectives

- 1) To study on the effect of different phase of titania on catalytic dehydration of ethanol to diethyl ether
- 2) To determine the stability of catalyst having the highest catalytic properties

### 1.4 Research scopes

- 1) Incipient wetness impregnation method was used for catalyst preparation
- 2) Proportion of anatase to rutile of titania support was varied upon 13.5 wt% of tungsten loading
- 3) Proportion of titania phase are including 0, 25, 50, 75 and 100 wt% of rutile
- 4) Catalysts that obtained after impregnation were characterized by SEM/EDX, XRD, N<sub>2</sub>-physisorption, NH<sub>3</sub>-TPD technique.
- 5) Dehydration reaction was performed under atmospheric pressure and temperature interval range of 200 – 400 °C.
- 6) Analysis of all products by gas chromatography (GC) with FID.

### 1.5 Expected benefits

- 1) Find the appropriate proportion of titania phase for WO<sub>3</sub>/TiO<sub>2</sub> catalyst on catalytic dehydration of ethanol to diethyl ether.
- 2) Understand causes of the catalytic dehydration of ethanol to diethyl ether due to different phase of titania.
- 3) The efficiency of the obtained catalyst can be used as references for the industry sector.

## CHAPTER 2

### THEORY AND LITERATURE REVIEWS

#### 2.1 Ethanol

Ethanol is organic compounds that are raw material to produce many valuable substances. In the present with the requirement to conserve the environment and reduce the use of fossil fuels, so ethanol produced from natural raw materials such as molasses, starch, etc. The most commonly used fermentation process to produce ethanol and the products called “bioethanol”.

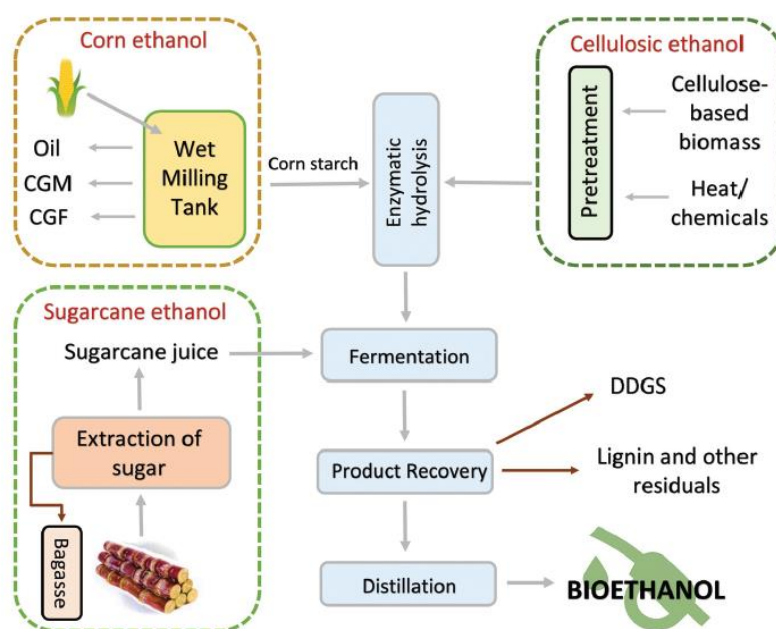


Figure 4 Diagram for bioethanol production from natural sources [16]

#### 2.2 Ethanol dehydration

In addition, the widely use of hydrocarbon cracking processes in petrochemical industry for the production of ethylene which is main product, the ethanol dehydration reaction can also produce ethylene as well by selecting appropriate temperature and catalysts.

Many products were produced by the dehydration reaction that uses ethanol as raw material. The main product obtained is ethylene. However, the ethanol dehydration reaction can also produce ethyl ether as byproducts in different pathway.

Both pathways will be competitive occurrence. The reaction for ethylene formation requires high temperature due to the reaction is endothermic reaction as shown in the reaction equation (1), while the diethyl ether formation requires lower temperature due to the reaction is exothermic reaction as shown in reaction equation (2) as below.

Dehydration of ethanol with bimolecular elimination mechanism (E2) to produce ethylene:



Dehydration of ethanol with bimolecular nucleophilic substitution mechanism ( $\text{S}_{\text{N}}2$ ) to produce diethyl ether:



Apart from ethylene and diethyl ether, the ethanol dehydration reaction also produces byproduct is a variety of products such as acetaldehyde by dehydrogenation reaction, methane, ethane, propylene and butylene [11, 12].

### 2.3 Catalysts

Catalyst helps to reduce activation energy, making reactions easier and faster. After the reaction, the catalyst will return to its original form and not as a composition in molecules of the products.

Currently, various catalysts were used in many processes for increasing chemical reaction rate. In order to use the catalyst, it is necessary to select a catalyst that quickly react, provide high products and good catalytic properties. Considerations for catalyst selection shall be determine the properties of the catalyst such as surface area, particle size, pore diameter, pore volume, acidity. For example, catalyst with higher surface area given higher conversion than lower surface area [14].

In addition, highly stable catalyst can be reused many times by performance and efficiency does not change, which causes the production cost to decrease as well.

The ethanol dehydration reaction to ethylene and diethyl ether will react well. The reaction requires an acidic catalyst that effect to high selectivity and catalytic activity. Many catalysts were used over supports such as W, Ca, Ru, Pd, etc [12, 17].

Tungsten (VI) oxide ( $\text{WO}_3$ ) is an oxide component of tungsten that has Brønsted acidity property. So, it is active material and high activity for acid-catalytic processes

that widely uses in many processes including catalytic dehydration reaction of ethanol. The insertion of  $WO_3$  assist to increase amount of active site contained in the supported catalysts and distribution of Brønsted acid sites that lead to higher activity [14]. In addition to increase activity, tungsten also helps to make higher stability in catalysts and prevents the reaction of acetaldehyde and high molecular hydrocarbon production [14, 17].

## 2.4 Titanium (IV) oxide ( $TiO_2$ )

The catalyst is coated on the support. Due to the high porosity support, the reaction is improved by catalysts can be distributed on a large amount porosity in supports. There are many types of support. The methods used in preparation of supported catalysts, such as wet impregnation, incipient impregnation, dry impregnation method, etc.

Titania has many phases, namely rutile, anatase and brookite, but the most commonly used is anatase and rutile phase. Rutile and anatase have a tetragonal structure, while brookite has an orthorhombic structure. Rutile is very stable. Anatase and brookite are metastable because the phase can be changed to rutile when calcination at temperatures above  $500\text{ }^\circ\text{C}$  [18]. and can be examined by use XRD Techniques to analyze the titania phase by pure anatase phase with peak patterns at 25, 38 and 48 degree of  $2\theta$  [15].

Titania is used as a support in heterogeneous catalyst due to thermal stability and mechanical resistance [17].

## 2.5 Incipient wetness impregnation

Interpenetration of precursors into the supports is important factor that effects to synthesis of heterogeneous catalysts. There are many techniques for interpenetration, for example dry impregnation, incipient wetness impregnation and wet impregnation that depend on solution volume and pore volume of the supports.

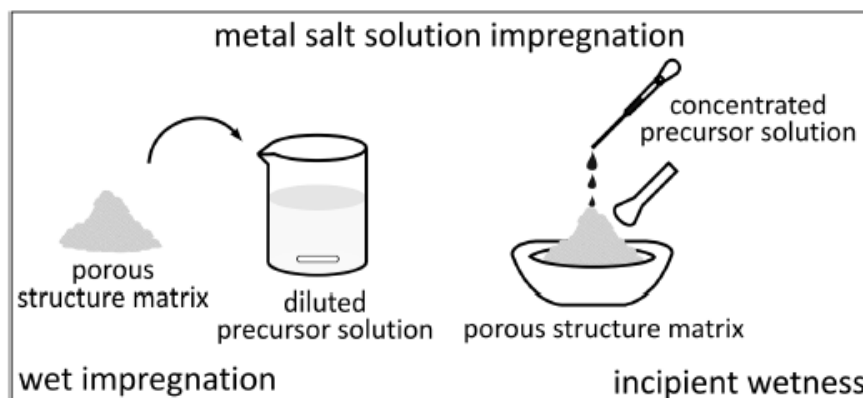


**Figure 5** Schematic of wet impregnation and incipient wetness impregnation techniques

The technique that is normally used in the synthesis of catalysts is incipient wetness impregnation by using solution of precursors in the volume that is equal to the pore volume of the supports so that the maximum precursor content can interpenetrate into pore of the supports. After interpenetrating, the supported catalysts were dried to remove water and eliminate the remaining volatile components by calcination [19, 20].

## 2.6 Literature reviews

The study of Phung et al. giving the data that selectivity of diethyl ether and ethylene are upon active site using in the dehydration reaction. For diethyl ether prefers low temperature than ethylene in the reaction. Besides, they found the active surface intermediates is ethoxy groups [13, 21].

Phung et al. [14] studied on the effect of  $WO_3$  addition into various supports for example titania ( $TiO_2$ ) and Zirconia ( $ZrO_2$ ) that effect on the supported catalysts and catalytic properties. For  $WO_3/TiO_2$  catalysts of Phung et al. were synthesized by impregnating. As a result, the amount of active site contained in the catalysts will be higher after  $WO_3$  insertion, which assists to produce Brønsted acid sites as well. So, the insertion of  $WO_3$  is good for the ethanol dehydration reaction and obviously giving high catalytic activity when compared with titania without tungsten and preventing the

occurrence of acetaldehyde and high molecular hydrocarbon production by acting as the poison [14].

Due to preparation of supports in different method effects to properties of catalysts and catalytic properties. Tresatayawed et al. [17] determine  $WO_3/TiO_2$  catalysts over ethanol dehydration to diethyl ether and ethylene by different methods are sol-gel and solvolthermal methods for preparation of titania supports and determine the reaction between 200 – 400 °C. Solvolthermal is better than sol-gel and giving the highest yield of diethyl ether ca. 26% at 250 °C and ethylene ca. 77% at 400 °C. Preparation of supports by solvolthermal makes high acidity and high surface area in catalysts [17].

Catalytic activity depends on condition in reaction, composition of catalysts, preparation, distribution of metals and supports were used, so the changing of support is one of the important factors on catalytic properties. Jongsomjit et al. [15] interested in various crystalline phase of titania in acting as the supports. In changing of crystalline phase of titania supports greatly effect to the physical and chemical properties, XRD techniques was used to determine crystalline phase changing. The results show that rutile phase not exceed 19% can be increasing selectivity of CO hydrogenation and the highest activity of CO Hydrogenation in this study occurs from 19% rutile phase. However, if rutile phase over 19% will lead to decreased selectivity [15].

A good catalyst should provide a high catalytic activity. One of the important factors is the distribution of metal on support. The research of Jongsomjit et al. [22] studied the differences in the distribution of Co on different phase of titania supports. The results show that Co Can be distributed on the surface of rutile phase is better than anatase phase by using TEM technique to determine [22].

P25 was studied on physical properties by calcination in different temperatures (500, 700 and 900 °C). The result shows that the increased temperature causes the intensity of the rutile peak increases and temperature is over 500 °C, the anatase peak decreases significantly while the rutile intensity peak increases. In addition, the

untreated P25 has a higher surface area than the P25 treated. Calcination over 500 °C has a significant effect on the anatase and rutile phase. Increasing in temperature, particle size and pore size also increase [23].

Kerdnoi et al. [24] determine in  $\text{WO}_3/\text{TiO}_2$  catalysts in different phase of titania that consist of anatase and rutile. The results show that catalysts with anatase supports giving the highest yield of diethyl ether and ethylene ca 27.4% and 10.6% respectively for catalytic dehydration reaction of ethanol at 300 °C. Because of the surface area of the catalyst that uses the anatase phase as a support, rather than leading to better dispersion of tungsten which is acid site.

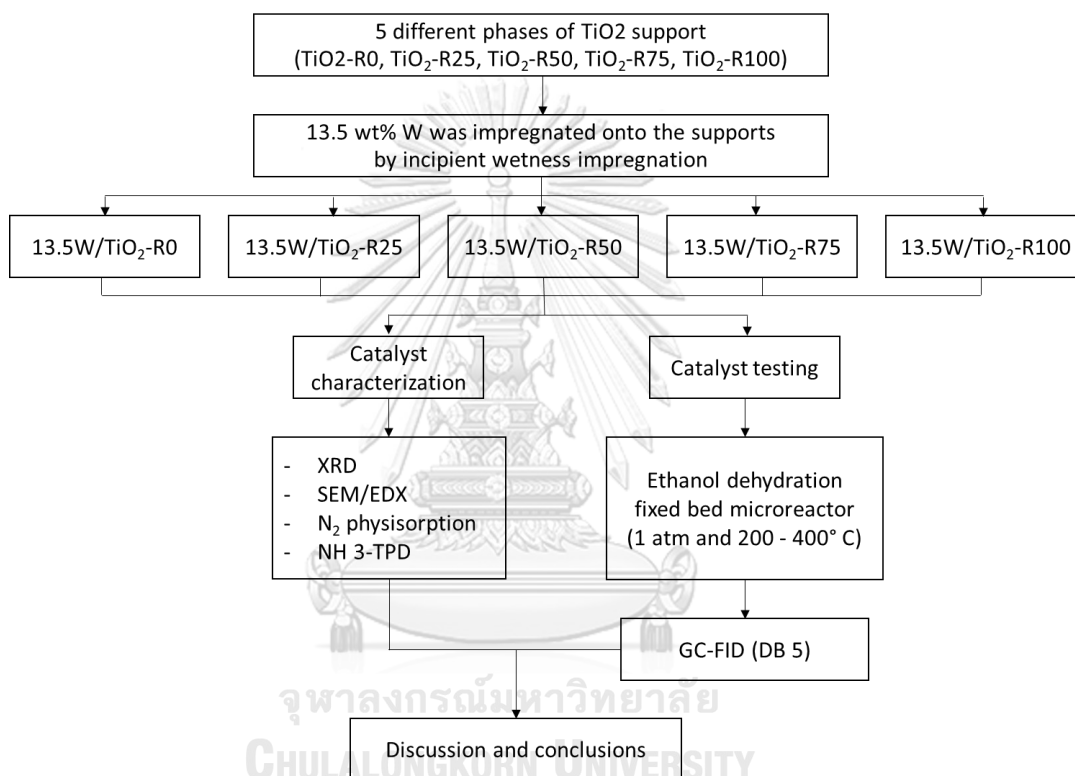


## CHAPTER 3

### EXPERIMENTS

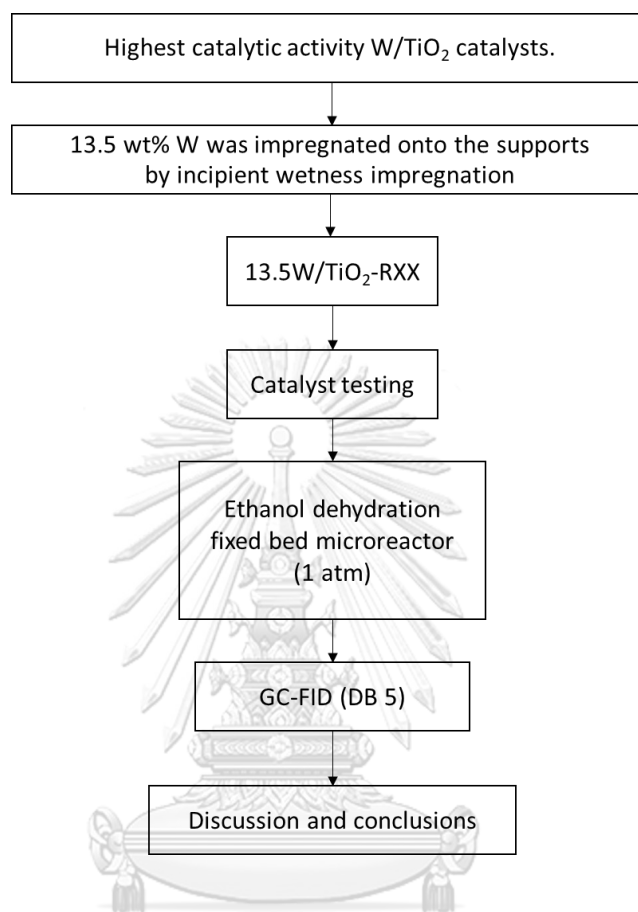
#### 3.1 Research methodology

**Part I:** The characteristic and catalytic activity of  $\text{WO}_3/\text{TiO}_2$  catalysts with different phases of  $\text{TiO}_2$  (R0, R25, R50, R75 and R100)





**Part II:** Stability of  $\text{WO}_3/\text{TiO}_2$  catalyst having the highest catalytic activity (from Part I)



### 3.2 Catalyst preparation

#### 3.2.1 Chemicals

- Titanium (IV) oxide or titania ( $\text{TiO}_2$ ): anatase, rutile from Sigma-Aldrich
- Tungsten (VI) chloride (99.9+% metals) from Sigma-Aldrich
- De-ionized water

#### 3.2.2 Preparation of $\text{WO}_3/\text{TiO}_2$ catalysts with different phases

Tungsten content of 13.5 wt% was used as precursor with dissolve in deionized water and impregnated onto titania support in different phase ( $\text{TiO}_2\text{-R0}$ ,  $\text{TiO}_2\text{-R25}$ ,  $\text{TiO}_2\text{-R50}$ ,  $\text{TiO}_2\text{-R75}$  and  $\text{TiO}_2\text{-R100}$ ) by incipient wetness impregnation. Then, they were dried at 110 °C for overnight, and calcined at 500 °C for 3 hours.

### 3.2.2 Catalyst nomenclature

The nomenclature used for the catalysts in this study is as follows:

$\text{WO}_3/\text{TiO}_2\text{-RX}$  : X refers to portion (mol%) of titania phase

## 3.3 Catalyst characterization

### 3.3.1 X-ray diffraction (XRD)

XRD analyzer by SIEMENS D-5000 X-ray diffractometer with  $\text{Cu K}\alpha$  ( $\lambda = 1.54439 \text{ \AA}$ ) was used to determine crystalline phase of catalyst in the range of  $2\theta = 20^\circ - 80^\circ$ .

### 3.3.2 Scanning electron microscope (SEM) and energy dispersive X-ray spectroscopy (EDX)

JEOL JSM-5800LV model for SEM was used to display surface morphology of catalyst in 3D and using Link Isis series 300 program for XRD mapping to examine amount of distribution of each element on catalyst.

### 3.3.3 $\text{N}_2$ physisorption

Before  $\text{N}_2$  physisorption (multipoint) analyzing, all samples were dried to eliminate impurities and vaporize water. Micrometitics ASAP 2010 was used to analyze adsorption-desorption isotherm. The BET method was applied to determine total specific surface area (BET surface area) and the BJH method was used to determine total pore volume, pore size diameter.

### 3.3.4 Ammonia temperature-programmed desorption ( $\text{NH}_3$ -TPD)

It was conducted using Micromeritics Chemisorp 2750 Pulse Chemisorption System to determine acidity of catalyst. All catalyst samples and quartz wool were packed in the U tube glass, and then were preheated at  $500^\circ\text{C}$  under helium flow. After that 15% of  $\text{NH}_3/\text{He}$  was used to saturate the sample. Finally, the catalyst samples were desorbed under helium flow.

### 3.4 Reaction study of ethanol dehydration

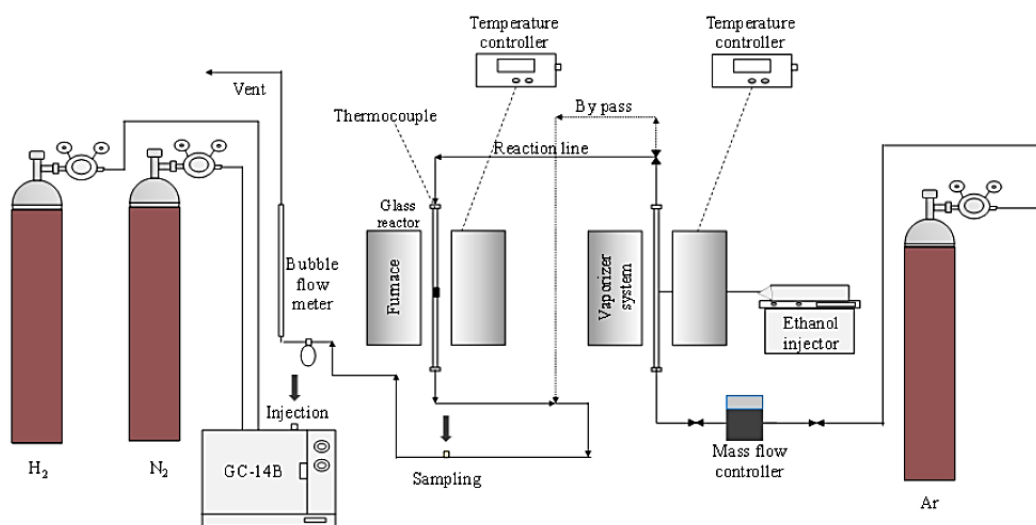


**Figure 6** Experimental set up for reaction test

Fixed-bed microreactor was used for the catalytic dehydration of ethanol and the experimental set-up apparatus is shown in **Figure 6**

#### 3.4.1 Temperature controller

Temperature controller was used for controlling the temperature of vaporizer, reactor and heating tape which can be identified and monitor the actual temperature in the equipment. The temperature controller can be controlled up to 400 °C.

#### 3.4.2 Mass flow controller

Mass flow controller controls nitrogen flow rate that acts as a carrier into the reactor.

#### 3.4.3 Syringe pump

Ethanol was fed in the syringe pump to inject in the vaporizer with 1.45 ml/h.

#### 3.4.4 Vaporizer

Due to ethanol in this research is liquid phase, so vaporizer was used for heating ethanol liquid phase to vapor phase at 120 °C under atmospheric pressure to react in the reactor.

### 3.4.5 Reactor

The fixed bed microreactor has an internal diameter of 7 mm and length of 330 mm. It is made from borosilicate glass that is heat resistant. The catalytic dehydration of ethanol occurs at the middle of the reactor which packed the catalyst and quartz wool.

### 3.4.6 Heating tape

Heating tape prevent the condensation in the process by covering on the pipeline.

### 3.4.7 Gas chromatography

Shimadzu GC14B (DB5) is a gas chromatography analyzer. Due to all products of this research are organic compounds, therefore the flame ionization detector (FID) signal was used for analyzing all products.

## 3.5 Reaction test

Fixed-bed microreactor was used for catalytic ethanol dehydration by the obtained  $\text{WO}_3/\text{TiO}_2$  catalyst 0.1 g in the middle of the reactor and quart wool 0.015 g and 0.005 g at below and above of catalyst respectively. After that preheated catalyst at 200 °C for 1 h to remove water and impurities on catalyst by nitrogen flowrate 56.4 ml/min. Then, ethanol was fed by a single syringe pump with flow rate 0.397 ml/h to vaporize at 120 °C for 1 h ( $3.13 \text{ h}^{-1}$  WHSV). Finally, catalytic ethanol dehydration (Temperature Program) was performed under condition of atmospheric pressure and temperature interval range is 200 - 400°C and all products in each condition were analyzed by GC-FID. For part 2 of the study, catalytic ethanol dehydration was tested for stability by reaction test with time on stream

## 3.6 Analysis and Calculation

The catalytic activities (conversion, selectivity and yield) were calculated as follows;

## 3.6.1 Ethanol conversion

$$\text{Ethanol conversion (\%)} = \frac{(\text{mol of ethanol in feed} - \text{mol of ethanol in product})}{\text{mol of ethanol in feed}} \times 100$$

## 3.6.2 Product selectivity

$$\text{Product selectivity (\%)} = \frac{\text{mol of each product}}{\text{mol of total products}} \times 100$$

## 3.6.3 Product yield

$$\text{Product yield (\%)} = \frac{\text{ethanol conversion} \times \text{selectivity of each product}}{100}$$

## 3.6.4 Rate of reaction

$$\text{Rate} = \frac{F_{A0} \times X}{W}$$

## 3.7 Research plan

Table 1 Schedule of the research plan

Research plan	2018		2019												
	Nov	Dec	Jan	Feb	Mar	Apr	May	Jun	Jul	Aug	Sep	Oct	Nov	Dec	
Studied about the theory related to ethanol dehydration reaction and their	←					→									
Considered the variables associated with the research.				←	→										
Prepared 13.5W/TiO <sub>2</sub> catalysts with different phases of titania (R0, R25, R50, R75, R100)						←	→								
Characterized all supports and 13.5W/TiO <sub>2</sub> catalysts with different phases of titania.							←	→	→						
Studied the catalytic activities via ethanol dehydration reaction.							←	→	→	→					
Studied the stability of the highest catalytic activities catalyst via ethanol dehydration										←	→	→			
Analyzed, discussed and concluded the obtained results.								←	→	→	→	→			
Prepared the report for presentation.											←	→	→	→	→

## CHAPTER 4

### RESULTS AND DISCUSSION

In this chapter, the results and discussion of  $WO_3/TiO_2$  catalysts are determined on characteristics and catalytic activities. All catalysts were prepared by incipient wetness impregnation as mentioned in the previous chapter. The results and discussion are divided into 3 parts. The first part describes the characteristics and catalytic activity of  $WO_3/TiO_2$  catalysts with different phases of  $TiO_2$  in ethanol dehydration reaction under vapor phase of ethanol with temperature program at temperature range between 200 °C and 400 °C. All catalysts were characterized by using various characterization techniques including X-ray diffraction (XRD), scanning electron microscope (SEM) and electron dispersive X-ray (EDX) spectroscopy,  $N_2$ -physisorption and temperature programmed desorption of ammonia ( $NH_3$ -TPD). The second part describes the catalytic activity of  $WO_3/TiO_2$  catalysts, which give the best catalytic activities at suitable temperature in the ethanol dehydration reaction under vapor phase of ethanol with time on stream to diethyl ether and ethylene and the characteristic after performed the reaction. The final part shows the comparison of catalysts for DEE and ethylene synthesis and their catalytic activity.

## Part I: The characteristic and catalytic activity of $\text{WO}_3/\text{TiO}_2$ catalysts with different phases of $\text{TiO}_2$ (R0, R25, R50, R75 and R100)

$\text{WO}_3/\text{TiO}_2$  catalysts were prepared with 13.5 wt% tungsten onto titania supports in different phase compositions by incipient wetness impregnation and then studied both catalytic properties and performance in ethanol dehydration.

### 4.1.1 X-ray diffraction (XRD)

To identify the crystalline structure of the catalysts. The XRD patterns of all catalysts are illustrated in **Figure 7**.

Results show that the  $\text{WO}_3/\text{TiO}_2\text{-R0}$  catalyst containing only anatase phase of titania support displays the peaks of anatase phase at  $25^\circ$  (major),  $37^\circ$ ,  $38^\circ$ ,  $48^\circ$ ,  $54^\circ$ ,  $55^\circ$  and  $75^\circ$ , whereas  $\text{WO}_3/\text{TiO}_2\text{-R100}$ , which has only rutile phase of titania support exhibits rutile peaks at  $28^\circ$  (major),  $36^\circ$  and  $54^\circ$ . Moreover,  $\text{WO}_3/\text{TiO}_2\text{-R25}$ ,  $\text{WO}_3/\text{TiO}_2\text{-R50}$  and  $\text{WO}_3/\text{TiO}_2\text{-R75}$  catalysts, which contain a mixture of anatase and rutile at 25%, 50% and 75% of rutile phase, respectively, display both peaks of anatase and rutile phase. In addition, the rutile peak intensity increases and anatase peak intensity decreases as % of rutile phase was increased. In the catalyst preparation, the 13.5 wt% of W was impregnated onto each titania supports and it can be observed the W species with very low intensity of XRD peaks at  $22^\circ$ ,  $33^\circ$  and  $63^\circ$  in all catalysts.

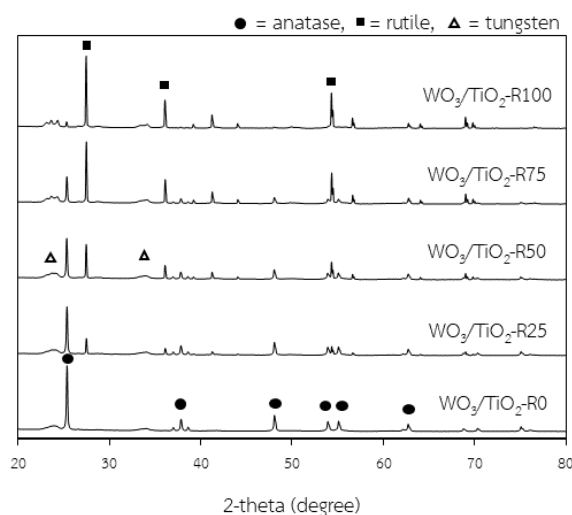


**Figure 7** XRD patterns of catalysts with different phase of  $\text{TiO}_2$

#### 4.1.2 Scanning electron microscope (SEM) and energy dispersive X-ray spectroscopy (EDX)

SEM shows morphology of each catalyst that is irregular shape as shown in **Figure 8**. It appears that the particle size of  $\text{WO}_3/\text{TiO}_2\text{-R0}$  is larger than those of the samples which contain anatase phase. In addition, the EDX mapping displays titanium (Ti), oxygen (O) and tungsten (W) atoms, which exhibited mainly good distribution on the external surface of catalysts in **Figures 9 to 13**. **Table 2** shows the percentage of weight for each element on the catalyst surface.

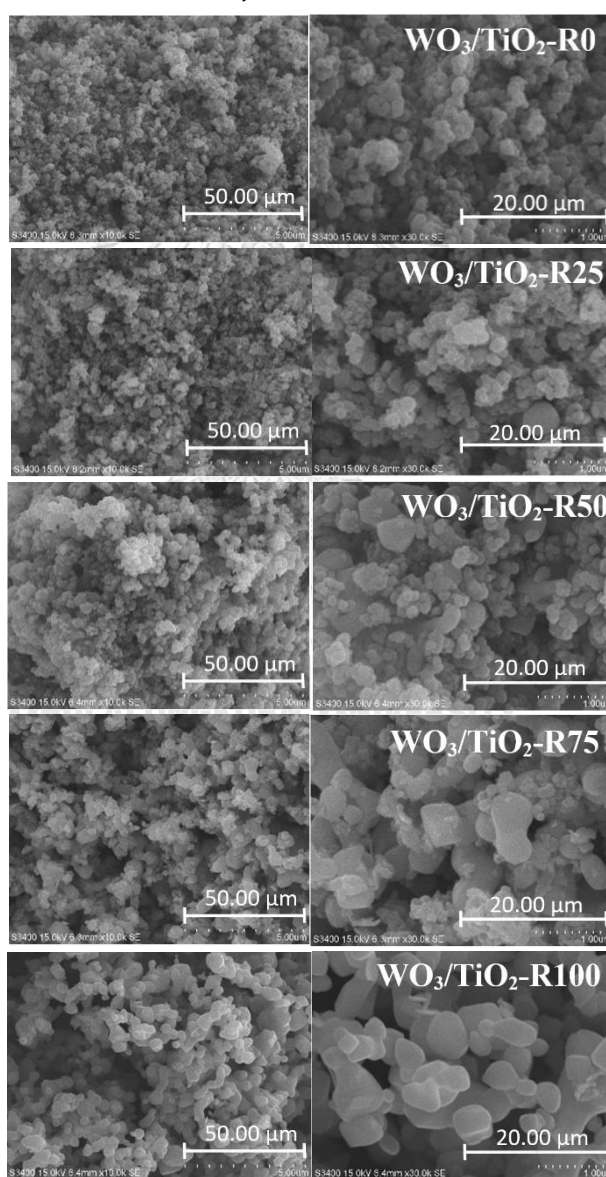


**Figure 8** SEM micrographs of all catalysts with different phase compositions of  $\text{TiO}_2$



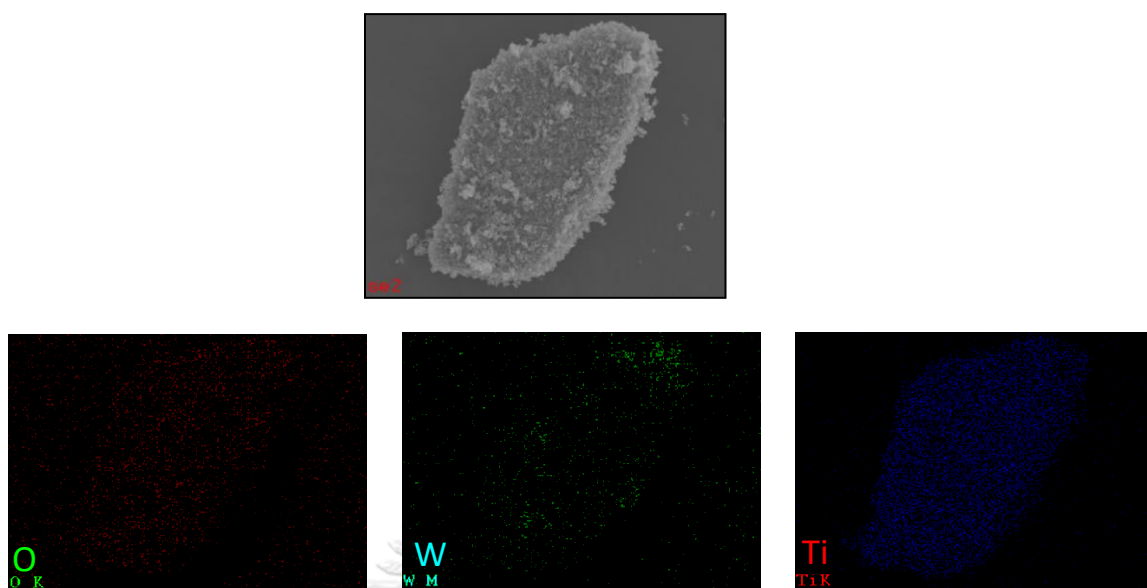


Figure 9 EDX mapping of  $\text{WO}_3/\text{TiO}_2\text{-R0}$

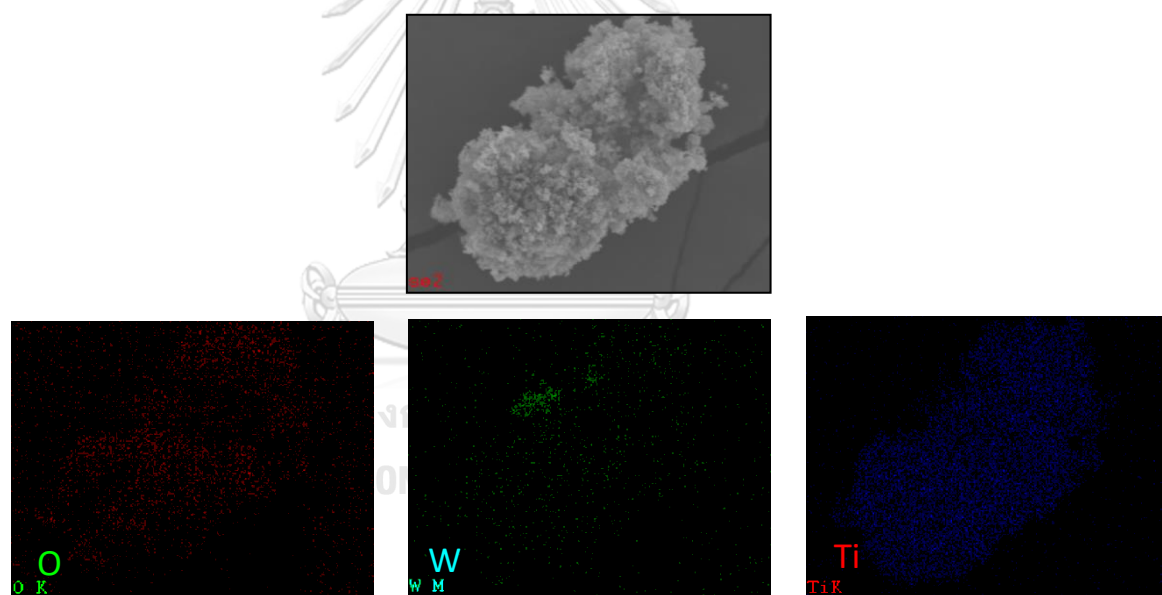


Figure 10 EDX mapping of  $\text{WO}_3/\text{TiO}_2\text{-R25}$

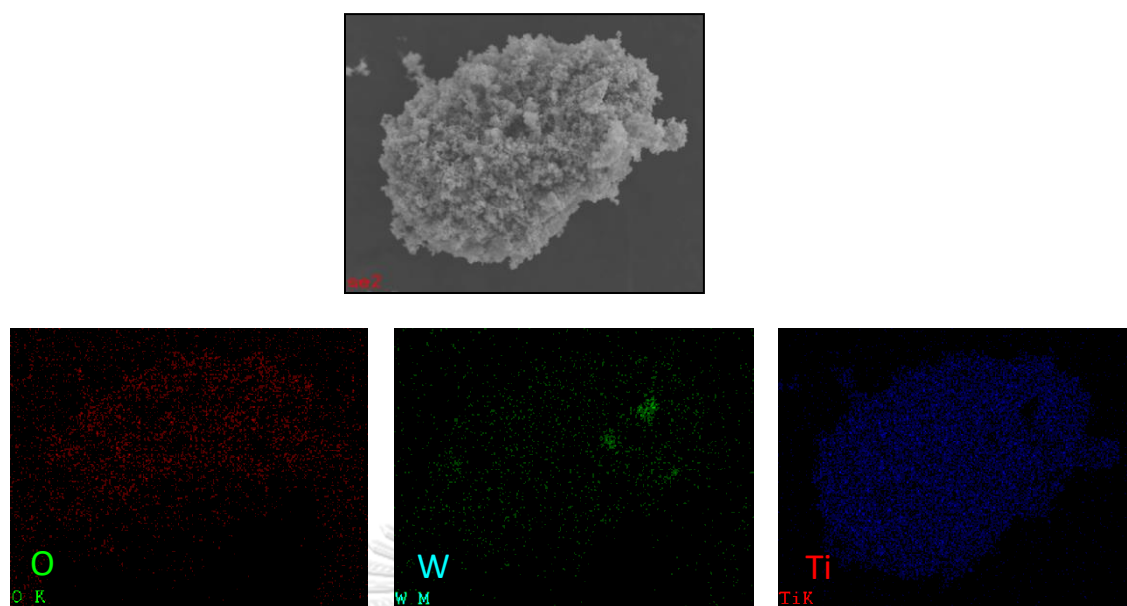


Figure 11 EDX mapping of  $\text{WO}_3/\text{TiO}_2$ -R50

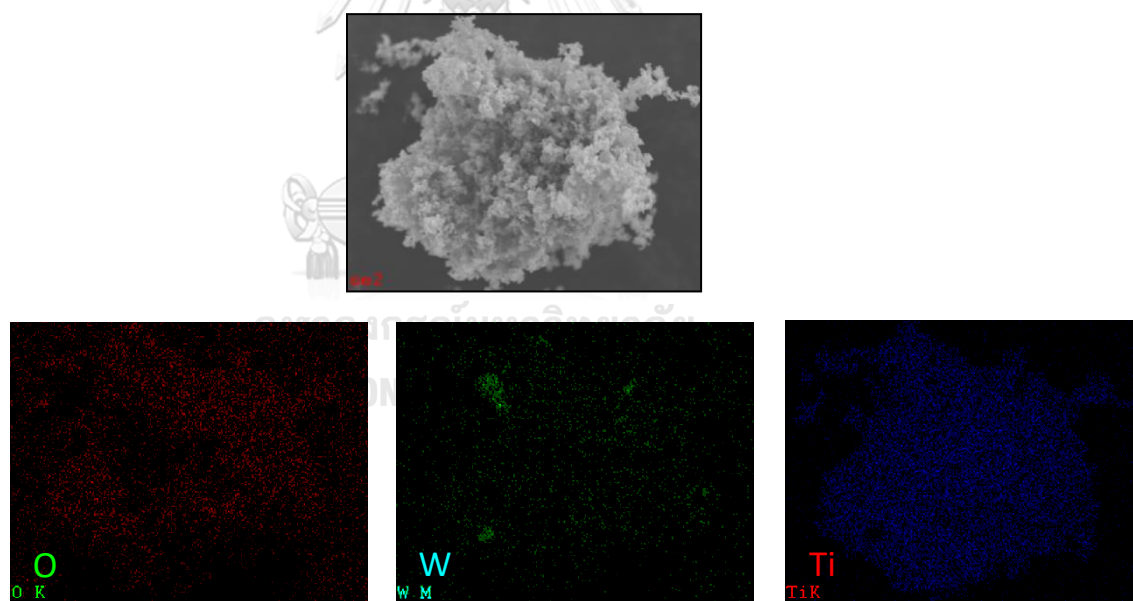


Figure 12 EDX mapping of  $\text{WO}_3/\text{TiO}_2$ -R75

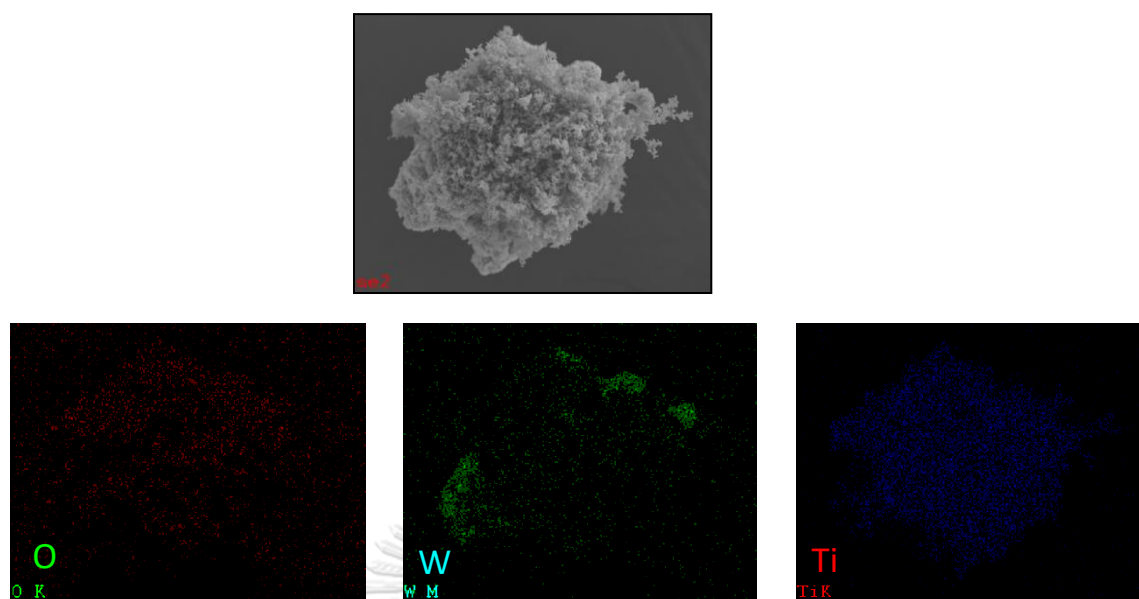


Figure 13 EDX mapping of  $\text{WO}_3/\text{TiO}_2\text{-R100}$

Table 2 The amount of elemental distribution on the catalyst surface

Catalysts	Amount of element on surface (wt%)			Amount of element on surface (at%)		
	O	W	Ti	O	W	Ti
$\text{WO}_3/\text{TiO}_2\text{-R0}$	40.3	5.7	53.9	68.6	0.9	30.6
$\text{WO}_3/\text{TiO}_2\text{-R25}$	41.6	5.2	53.1	69.9	0.8	29.7
$\text{WO}_3/\text{TiO}_2\text{-R50}$	43.7	3.9	52.4	71.0	0.6	28.5
$\text{WO}_3/\text{TiO}_2\text{-R75}$	43.8	4.0	52.2	71.1	0.6	28.3
$\text{WO}_3/\text{TiO}_2\text{-R100}$	39.7	10.6	49.7	69.3	1.6	29.1

Refer to the micrograph, **Tables 3** and **4** show the average width of particle sizes of  $\text{WO}_3/\text{TiO}_2$  of all catalysts, which are 1.68, 2.46, 3.28, 4.14 and 6.30 micron respectively, and the average length of particle sizes of  $\text{WO}_3/\text{TiO}_2$  of all catalysts are 1.96, 2.20, 3.40, 4.40 and 6.38 micron respectively. The results of calculation measured at random 50 particles and the histogram graphs display the distribution of particle sizes in **Figures 14 and 15**.

**Table 3** The average width of particle sizes of all catalysts

Catalysts	Width (micron)			
	Min	Max	Mean	S.D.
$\text{WO}_3/\text{TiO}_2\text{-R0}$	0.571	2.000	1.20	0.38
$\text{WO}_3/\text{TiO}_2\text{-R25}$	0.857	2.571	1.57	0.48
$\text{WO}_3/\text{TiO}_2\text{-R50}$	0.857	6.286	2.34	1.21
$\text{WO}_3/\text{TiO}_2\text{-R75}$	0.857	6.286	2.95	1.66
$\text{WO}_3/\text{TiO}_2\text{-R100}$	1.429	15.714	4.50	2.39

**Table 4** The average length of particle sizes of all catalysts

Catalyst	Length (micron)			
	Min	Max	Mean	S.D.
$\text{WO}_3/\text{TiO}_2\text{-R0}$	0.571	2.857	1.40	0.40
$\text{WO}_3/\text{TiO}_2\text{-R25}$	0.857	2.571	1.75	0.41
$\text{WO}_3/\text{TiO}_2\text{-R50}$	0.857	5.143	2.43	1.24
$\text{WO}_3/\text{TiO}_2\text{-R75}$	0.571	10.571	3.14	2.23
$\text{WO}_3/\text{TiO}_2\text{-R100}$	1.714	11.429	4.56	2.09

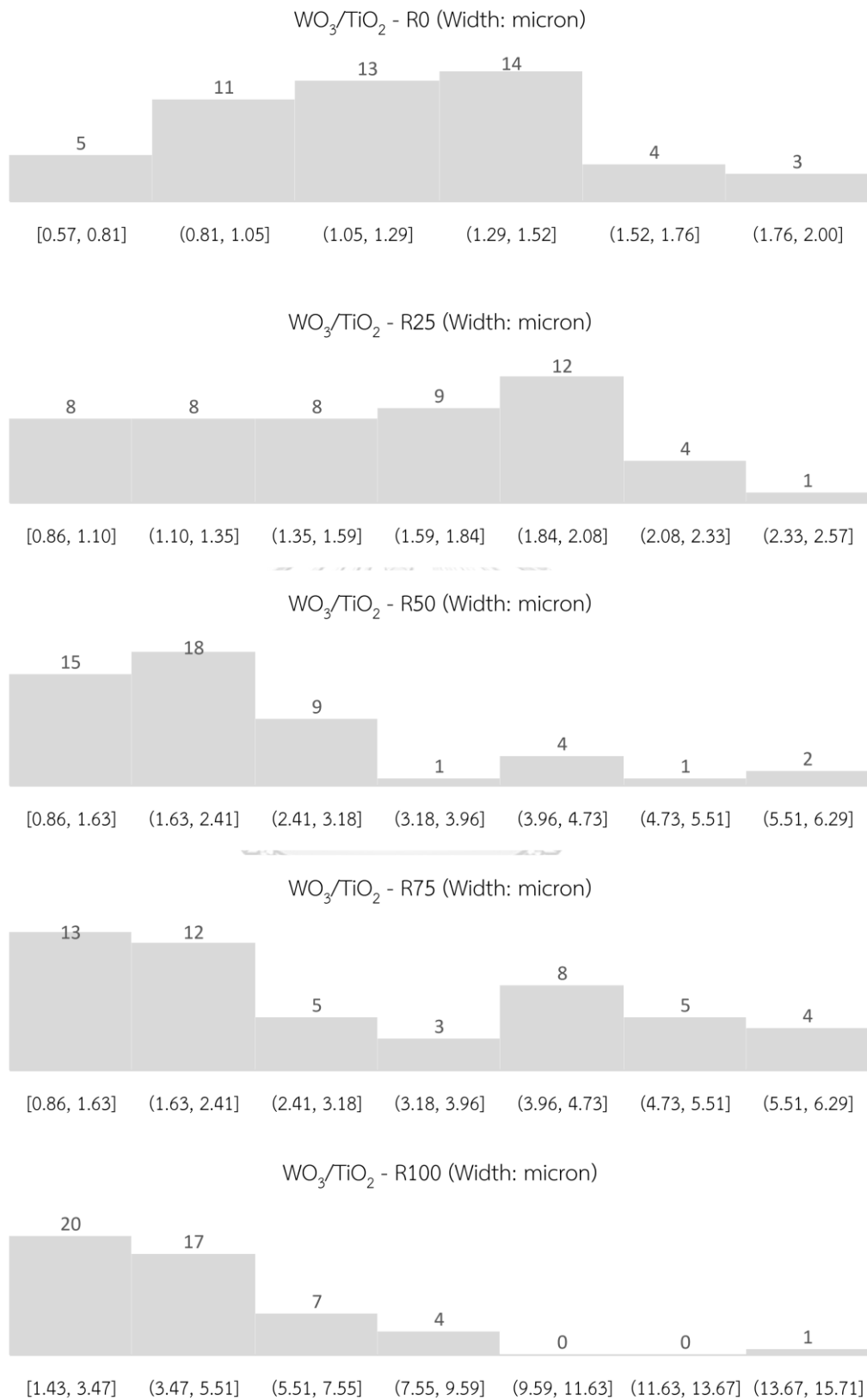


**Figure 14** Histogram graph on width of particle sizes of all catalysts

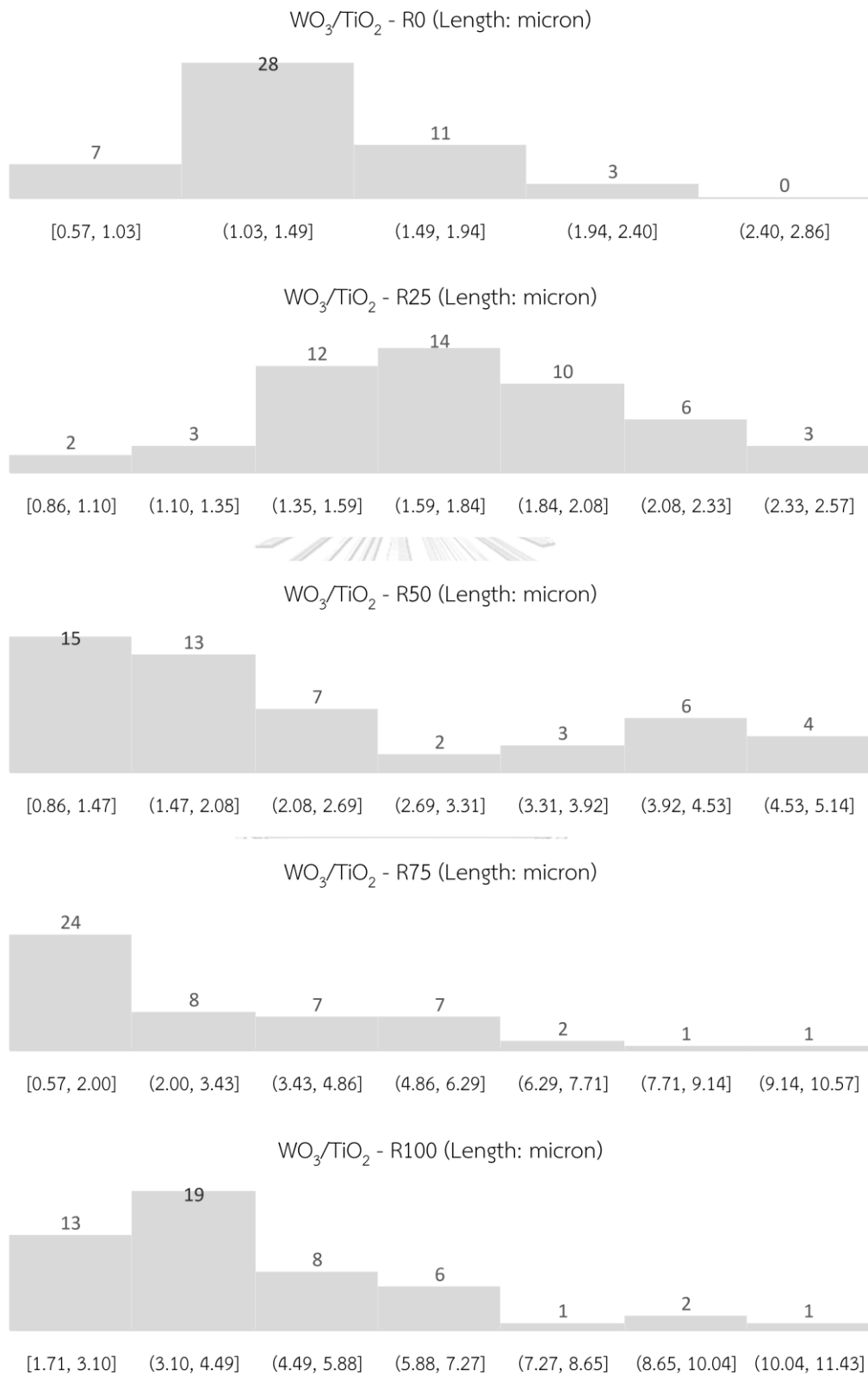


**Figure 15** Histogram graph on length of particle sizes of all catalysts

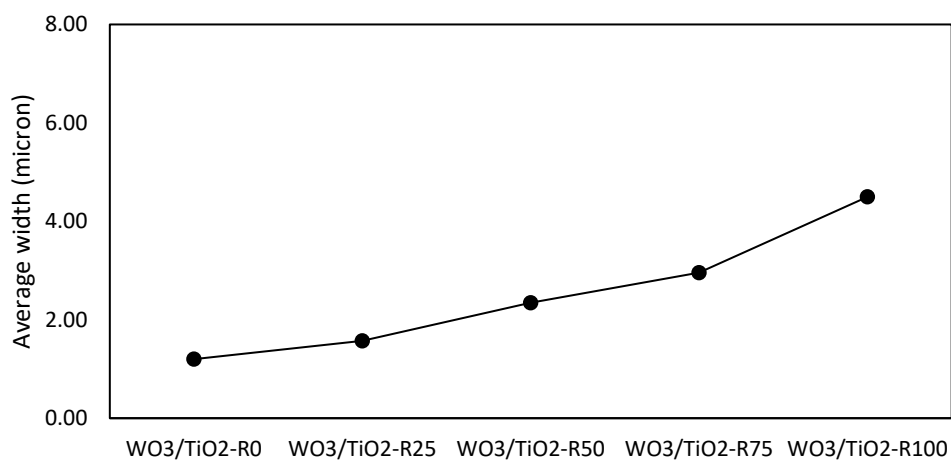


**Figure 16** The average width particle size of all catalysts

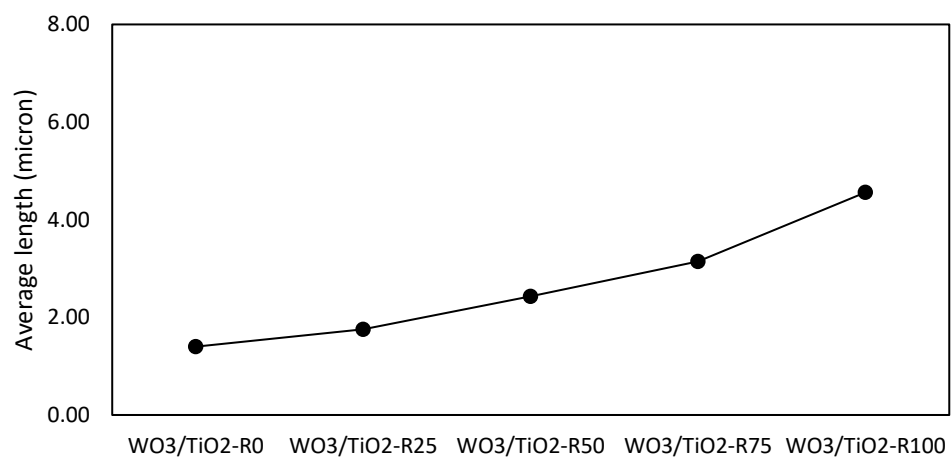


**Figure 17** The average length particle size of all catalysts

The average particle sizes of all catalysts are displayed in **Figures 16 and 17**. It can be concluded that rutile mixing in TiO<sub>2</sub> as supports of catalysts causes the particle size to increase.

#### 4.1.3 N<sub>2</sub> physisorption

BET surface area, pore volume and pore diameter of all catalysts with different portion of TiO<sub>2</sub> phase determined by N<sub>2</sub> physisorption are reported in **Table 5**. The WO<sub>3</sub>/TiO<sub>2</sub>-R0 catalyst, which contains only anatase phase of titania has the highest surface area (17.40 m<sup>2</sup>/g) and pore volume (0.06 cm<sup>3</sup>/g), while the WO<sub>3</sub>/TiO<sub>2</sub>-R100, which contains only rutile phase of titania has the lowest surface area (7.26 m<sup>2</sup>/g) and pore volume (0.03 cm<sup>3</sup>/g). The WO<sub>3</sub>/TiO<sub>2</sub>-R50 having equal amount of anatase and rutile phases, has the surface area between WO<sub>3</sub>/TiO<sub>2</sub>-R0 and WO<sub>3</sub>/TiO<sub>2</sub>-R100 as expected. However, the surface area close to WO<sub>3</sub>/TiO<sub>2</sub>-R100 (9.78 m<sup>2</sup>/g) and pore volume (0.04 cm<sup>3</sup>/g). It should be mentioned that the presence of rutile phase in titania support significantly affects the decreased surface area.

**Table 5** Textural properties of all catalysts with different phases of TiO<sub>2</sub>

Catalysts	BET Surface Area (m <sup>2</sup> /g)	Pore Volume (cm <sup>3</sup> /g)	Pore Size (nm)
WO <sub>3</sub> /TiO <sub>2</sub> -R0	17.4	0.06	16
WO <sub>3</sub> /TiO <sub>2</sub> -R50	9.8	0.04	17
WO <sub>3</sub> /TiO <sub>2</sub> -R100	7.3	0.03	22

N<sub>2</sub> adsorption-desorption isotherms at -196°C for the WO<sub>3</sub>/TiO<sub>2</sub>-R0, WO<sub>3</sub>/TiO<sub>2</sub>-R50 and WO<sub>3</sub>/TiO<sub>2</sub>-R100 catalysts are shown in **Figure 18**. It was found that all samples presented hysteresis loops indicating type IV isotherm according to IUPAC classification, which confirm the mesoporous structure. The pore size distributions (PSD) for the WO<sub>3</sub>/TiO<sub>2</sub>-R0, WO<sub>3</sub>/TiO<sub>2</sub>-R50 and WO<sub>3</sub>/TiO<sub>2</sub>-R100 catalysts are shown in **Figure 19**. All samples mainly have the average pore diameter range of 2–50 nm that were classified as mesoporous particles.



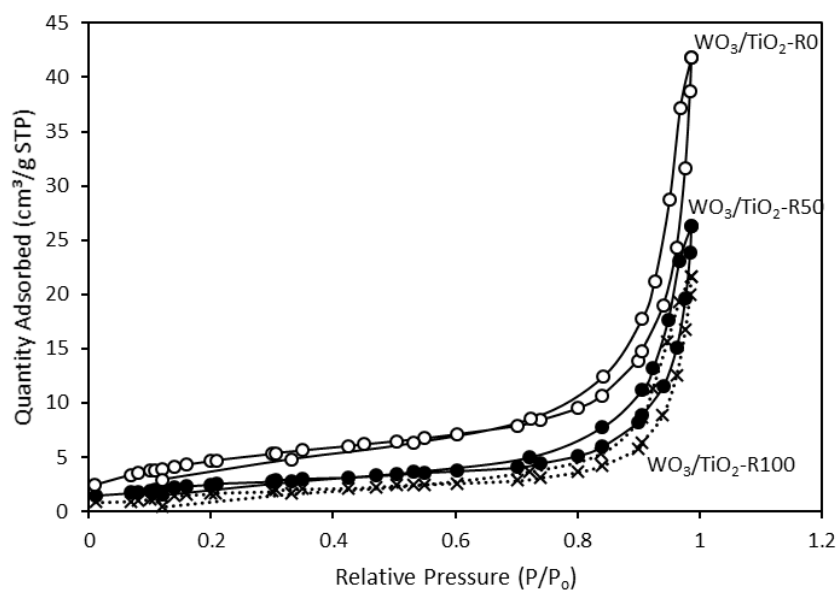


Figure 18  $N_2$  adsorption-desorption isotherms of  $WO_3/TiO_2$ -R0,  $WO_3/TiO_2$ -R50 and  $WO_3/TiO_2$ -R100 catalysts

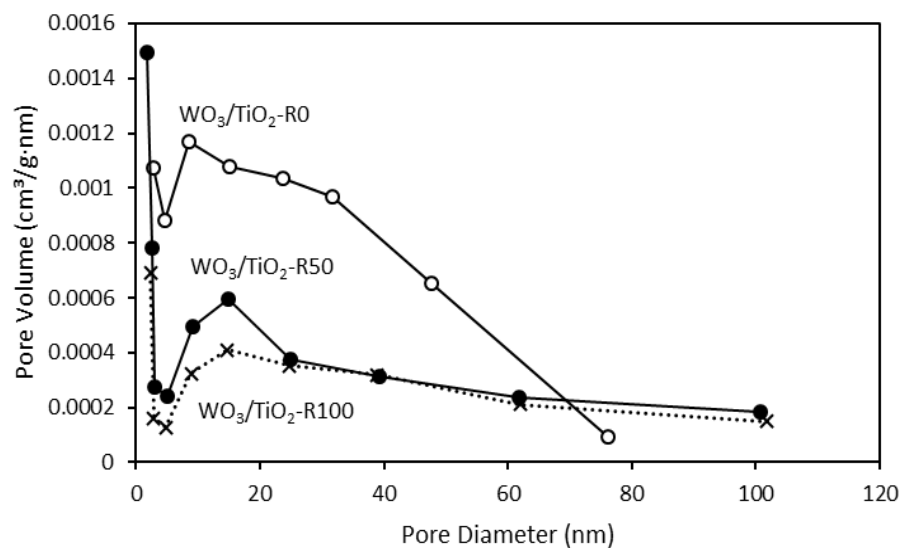
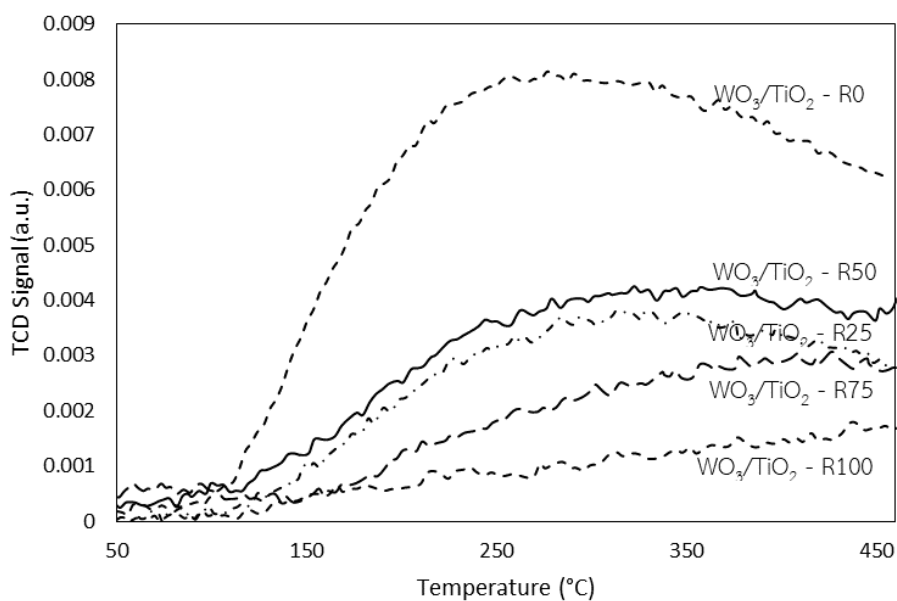


Figure 19 The pore size distribution of  $WO_3/TiO_2$ -R0,  $WO_3/TiO_2$ -R50 and  $WO_3/TiO_2$ -R100 catalysts

#### 4.1.4 Ammonia temperature-programmed desorption (NH<sub>3</sub>-TPD)

The amounts of acidity of all catalysts were characterized by using ammonia temperature-programmed desorption (NH<sub>3</sub>-TPD) and are displayed in **Figure 20**.



**Figure 20** NH<sub>3</sub>-TPD profiles of all catalysts with different phases of TiO<sub>2</sub>

Broad desorption peaks for all catalysts with different phase of TiO<sub>2</sub> excepting for WO<sub>3</sub>/TiO<sub>2</sub>-R100 were found in the temperature range from 150 to 500 °C, while WO<sub>3</sub>/TiO<sub>2</sub>-R100 did not have any desorption peaks. For desorption peaks at temperatures below 300 °C, they are represented by weak acid sites [17] while temperatures between 300 – 450 °C are represented by medium acid sites and more than 450 °C are represented by strong acid sites. The acidity of all catalysts was calculated from the area under broad peaks.

**Table 6** The amount of acidity of all catalysts with different phases of TiO<sub>2</sub>

Sample	NH <sub>3</sub> desorption (μmol/g cat)			Total acidity (μmol/g cat)	Weak to strong acid site ratio
	Weak	Medium	Strong		
WO <sub>3</sub> /TiO <sub>2</sub> - R0	788.5	271.9	928.1	1988.5	0.85
WO <sub>3</sub> /TiO <sub>2</sub> - R25	396.1	186.8	419.3	1002.2	0.94
WO <sub>3</sub> /TiO <sub>2</sub> - R50	549.7	167.2	564.6	1281.5	0.97
WO <sub>3</sub> /TiO <sub>2</sub> - R75	291.6	138.3	370.3	800.2	0.79
WO <sub>3</sub> /TiO <sub>2</sub> - R100	190.4	80.1	344.7	615.2	0.55

The total acid content of the catalysts with rutile phase of TiO<sub>2</sub> at 0%, 25%, 50%, 75% and 100% are shown in **Table 6** with values of 1988.5, 1002.2, 1281.5, 800.81, 615.2 μmol/g cat. In addition, WO<sub>3</sub>/TiO<sub>2</sub>-R50 gave the highest weak to strong acid ratio to 0.97. For WO<sub>3</sub>/TiO<sub>2</sub>-R0, WO<sub>3</sub>/TiO<sub>2</sub>-R25, WO<sub>3</sub>/TiO<sub>2</sub>-R75 and WO<sub>3</sub>/TiO<sub>2</sub>-R100, they gave the weak to strong acid ratio to 0.85, 0.94, 0.79 and 0.55, respectively.

#### 4.1.5 Reaction test

The catalytic dehydration reaction of ethanol at 200 to 400 °C was performed in the fixed-bed microreactor. The results are shown in **Figure 21**. For all catalysts no ethanol conversion at 200 °C was observed. Then, it can be seen that ethanol conversion apparently increased with increasing temperature for all catalyst samples up to 350 °C. However, all catalysts (except WO<sub>3</sub>/TiO<sub>2</sub>-R0) showed deactivation when the reaction temperature was raised to 400 °C. Therefore, the suitable temperature for these catalysts is 350 °C. The WO<sub>3</sub>/TiO<sub>2</sub>-R50 catalyst exhibited the highest ethanol conversion (84.0%) at 350 °C among other catalysts.

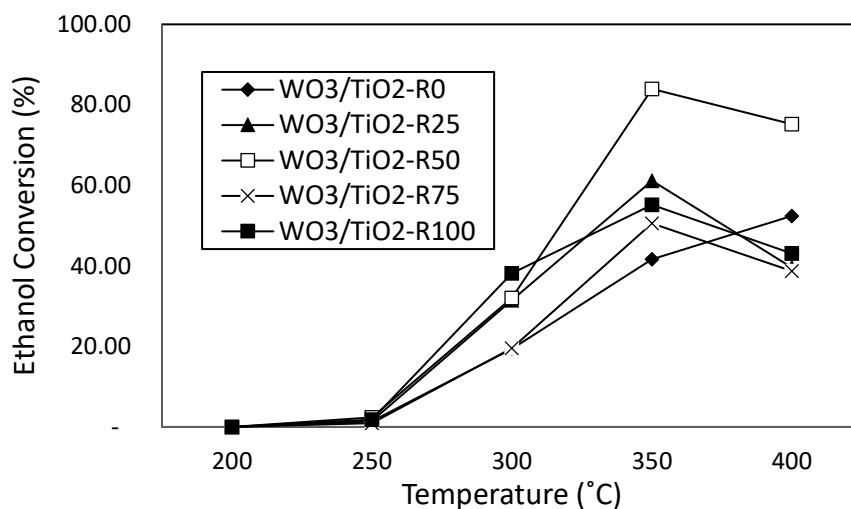


**Figure 21** Ethanol Conversion of all catalysts with different phase of TiO<sub>2</sub>

The product selectivity obtained from all catalysts are shown in **Figure 22**. It was found that diethyl ether (DEE) is a major product at 250 °C. The results also showed that at 250 to 350 °C, ethylene selectivity increased significantly with increasing temperature because it is endothermic reaction and slightly increased or decreased in the temperature interval range at 350 to 400 °C due to deactivation of catalysts. The WO<sub>3</sub>/TiO<sub>2</sub>-R100 catalyst at 400 °C and WO<sub>3</sub>/TiO<sub>2</sub>-R50 catalysts at 350 °C exhibited higher ethylene selectivity than other catalysts having similar ethylene selectivity of 95.7% and 94.8%, respectively. This is likely corresponding to the deactivation temperature for each catalyst.

Considering the diethyl ether formation, it is favored at lower temperatures because it is exothermic reaction. All catalysts gave the highest diethyl ether selectivity at 250 °C and decreased with increasing temperature. At below 350°C, WO<sub>3</sub>/TiO<sub>2</sub>-R0 and WO<sub>3</sub>/TiO<sub>2</sub>-R75 catalysts produced higher diethyl ether selectivity than other catalysts. Besides two products, acetaldehyde was also slightly formed as a byproduct at 300 °C.

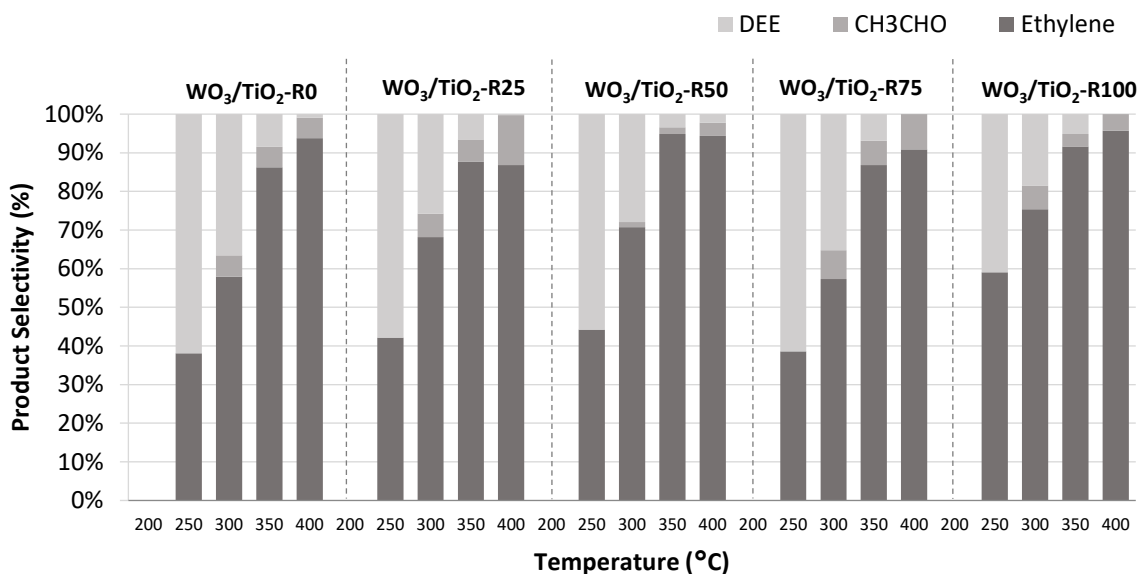


**Figure 22** Product selectivity of all catalysts with different phase of TiO<sub>2</sub>

The ethylene yield trend as a function of reaction temperature is reported in **Figure 23 (a)**. Ethylene yield was increased with increasing the reaction temperature because ethanol conversion and ethylene selectivity also increased at the temperature up to 350 °C. The WO<sub>3</sub>/TiO<sub>2</sub>-R50 catalysts at 350°C gave the highest ethylene yield of 79.6%.

From **Figure 23 (b)**, it shows the DEE yield of all catalysts increased with increasing the reaction temperature up to 300 °C. In addition, at 300 °C, WO<sub>3</sub>/TiO<sub>2</sub>-R50 catalyst gave the highest DEE yield (9.0%) compared with all catalysts and reaction temperatures. After that with increasing the reaction temperature, DEE yield decreased due to the lower DEE selectivity. Besides two products, acetaldehyde was slightly formed as a byproduct as shown in **Figure 23 (c)**.

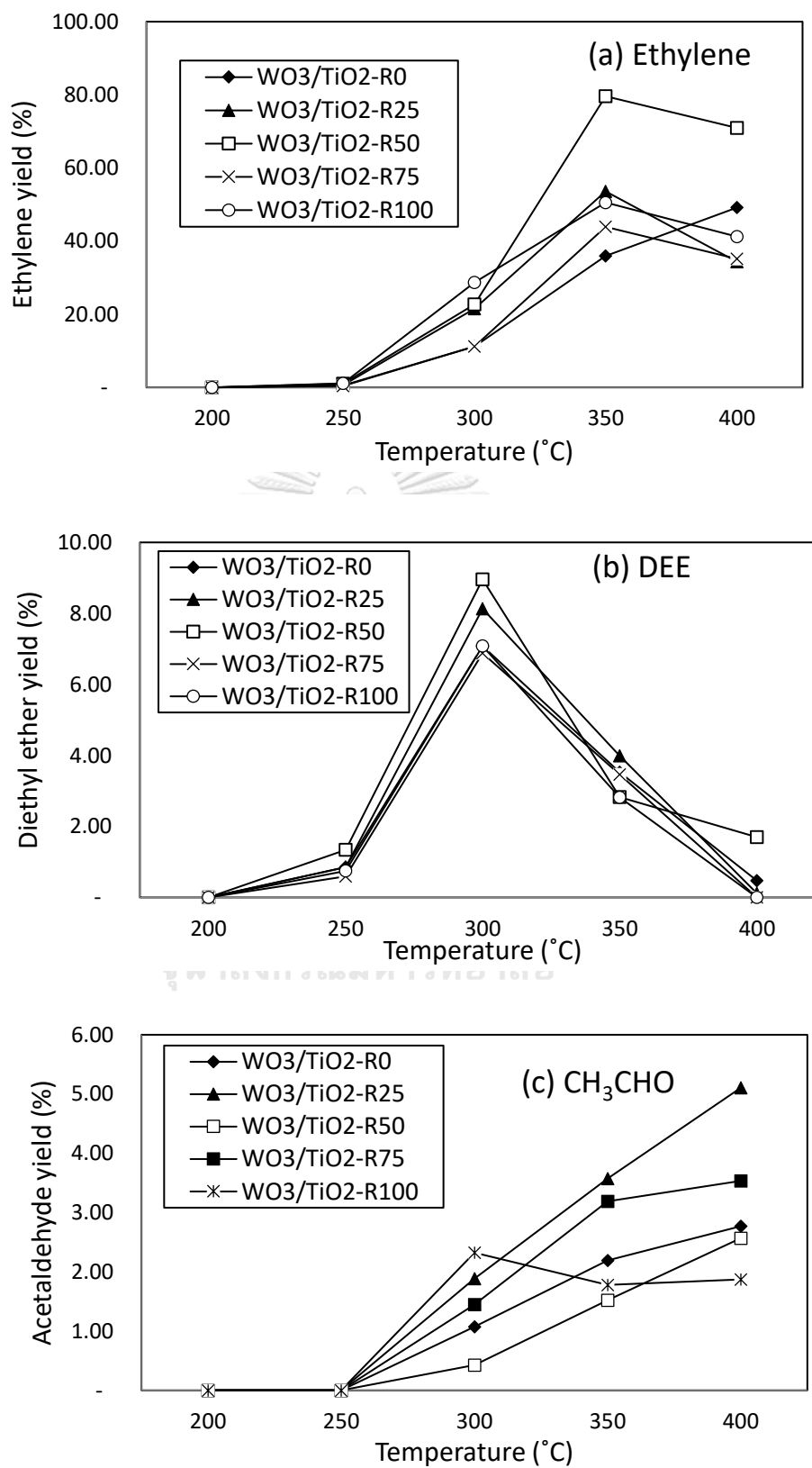


Figure 23 Product yields of all catalysts with different phase of TiO<sub>2</sub>

**Table 7** Ethanol conversion, product selectivity and product yield

Catalyst	Temperature (°C)	Ethanol Conversion (%)	Product Selectivity (%)			Product Yield (%)		
			Ethylene	CH <sub>3</sub> CHO	DEE	Ethylene	CH <sub>3</sub> CHO	DEE
WO <sub>3</sub> /TiO <sub>2</sub> -R0	200	0.0	0.0	0.0	0.0	0.0	0.0	0.0
	250	1.4	38.1	0.0	61.9	0.5	0.0	0.9
	300	19.4	57.9	5.5	36.6	11.2	1.1	7.1
	350	41.6	86.3	5.3	8.5	35.9	2.2	3.5
	400	52.4	93.8	5.3	0.9	49.2	2.8	0.5
WO <sub>3</sub> /TiO <sub>2</sub> -R25	200	0.0	0.0	0.0	0.0	0.0	0.0	0.0
	250	1.5	42.1	0.0	57.9	0.6	0.0	0.9
	300	31.5	68.2	6.0	25.8	21.5	1.9	8.1
	350	61.2	87.6	5.8	6.5	53.6	3.6	4.0
	400	39.6	86.8	12.9	0.3	34.4	5.1	0.1
WO <sub>3</sub> /TiO <sub>2</sub> -R50	200	0.0	0.0	0.0	0.0	0.0	0.0	0.0
	250	2.4	44.2	0.0	55.8	1.1	0.0	1.3
	300	32.1	70.7	1.3	27.9	22.7	0.4	9.0
	350	84.0	94.8	1.8	3.4	79.6	1.5	2.8
	400	75.2	94.3	3.4	2.3	71.0	2.6	1.7
WO <sub>3</sub> /TiO <sub>2</sub> -R75	200	0.0	0.0	0.0	0.0	0.0	0.0	0.0
	250	1.0	38.6	0.0	61.4	0.4	0.0	0.6
	300	19.5	57.4	7.4	35.2	11.2	1.4	6.9
	350	50.6	86.8	6.3	6.9	43.9	3.2	3.5
	400	38.7	90.9	9.1	0.0	35.1	3.5	0.0
WO <sub>3</sub> /TiO <sub>2</sub> -R100	200	0.0	0.0	0.0	0.0	0.0	0.0	0.0
	250	1.8	59.1	0.0	40.9	1.1	0.0	0.7
	300	38.1	75.3	6.1	18.6	28.7	2.3	7.1
	350	55.2	91.7	3.2	5.1	50.6	1.8	2.8
	400	43.1	95.7	4.3	0.0	41.2	1.9	0.0

The results as reported in **Table 7**, WO<sub>3</sub>/TiO<sub>2</sub>-R50 catalysts gave the highest ethylene and DEE yields for ethanol dehydration when compared with other catalysts. So, the portion of phase composition of titania support can affect the catalytic behavior of WO<sub>3</sub>/TiO<sub>2</sub> catalysts in the ethanol dehydration. WO<sub>3</sub>/TiO<sub>2</sub>-R50 catalyst exhibited the highest weak to strong acid ratio properties of catalysts among other

catalysts. The ratios are the factor leading to high activity for ethanol dehydration to DEE and ethylene of the catalyst due to the reaction prefers weak acids and dislikes strong acids. Therefore, the further study selects  $\text{WO}_3/\text{TiO}_2\text{-R50}$  catalyst to study the stability of the catalyst on ethanol dehydration reaction to DEE at 300 °C and to ethylene at 350 °C.

#### 4.1.6 Dispersive X-ray spectroscopy (EDX) for spent catalysts

Coke formation of  $\text{WO}_3/\text{TiO}_2$  catalysts with different phase of  $\text{TiO}_2$  after being used in the ethanol dehydration reaction at temperature in range of 200 – 400 °C was determined by measuring %carbon with EDX analysis. The results are displayed in

**Table 8**

**Table 8** The amount of %carbon in the spent catalysts

Catalysts	%Carbon
$\text{WO}_3/\text{TiO}_2\text{-R0}$	1.92
$\text{WO}_3/\text{TiO}_2\text{-R25}$	1.77
$\text{WO}_3/\text{TiO}_2\text{-R50}$	1.83
$\text{WO}_3/\text{TiO}_2\text{-R75}$	1.87
$\text{WO}_3/\text{TiO}_2\text{-R100}$	1.41

From the table, it was found that  $\text{WO}_3/\text{TiO}_2\text{-R0}$  gave the highest %carbon of 1.92% and  $\text{WO}_3/\text{TiO}_2\text{-R100}$  exhibited the lowest %carbon of 1.41%, while  $\text{WO}_3/\text{TiO}_2\text{-R25}$ ,  $\text{WO}_3/\text{TiO}_2\text{-R50}$  and  $\text{WO}_3/\text{TiO}_2\text{-R75}$  contained %carbon of 1.77%, 1.83% and 1.87%, respectively. Because coke formation is related to the total acidity of the catalysts, thus, catalysts with high total acidity also has high coke formation. Therefore, when focusing on the %carbon of  $\text{WO}_3/\text{TiO}_2\text{-R0}$  and  $\text{WO}_3/\text{TiO}_2\text{-R100}$ , the results were related to total acidity of catalysts that as mentioned above.



#### 4.1.7 Catalysts appearance

Appearance of catalysts with different phase of  $\text{TiO}_2$  was presented to observe the color change of before and after ethanol dehydration reaction. The appearance of fresh and spent catalysts with different phases of  $\text{TiO}_2$  is presented in **Figures 24 and 25**, respectively.



**Figure 24** The appearance of fresh catalysts with different phase of  $\text{TiO}_2$   
 (a)  $\text{WO}_3/\text{TiO}_2\text{-R0}$  (b)  $\text{WO}_3/\text{TiO}_2\text{-R25}$  (c)  $\text{WO}_3/\text{TiO}_2\text{-R50}$  (d)  $\text{WO}_3/\text{TiO}_2\text{-R75}$  (e)  $\text{WO}_3/\text{TiO}_2\text{-R100}$

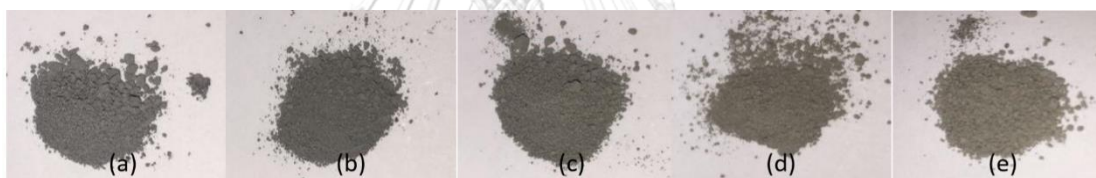


**Figure 25** The appearance of spent catalysts with different phase of  $\text{TiO}_2$   
 (a)  $\text{WO}_3/\text{TiO}_2\text{-R0}$  (b)  $\text{WO}_3/\text{TiO}_2\text{-R25}$  (c)  $\text{WO}_3/\text{TiO}_2\text{-R50}$  (d)  $\text{WO}_3/\text{TiO}_2\text{-R75}$  (e)  $\text{WO}_3/\text{TiO}_2\text{-R100}$

The presence of tungsten in surface of catalysts makes the appearance of all fresh  $\text{WO}_3/\text{TiO}_2$  catalysts turn into yellow. After all catalysts were performed in ethanol dehydration reaction, the spent catalysts were observed and they were presented grey color due to coke formation that corresponding with carbon existing in EDX analysis.

#### 4.1.8 X-ray diffraction (XRD) for spent catalysts

XRD patterns of  $\text{WO}_3/\text{TiO}_2$  catalysts with different phase of  $\text{TiO}_2$  containing 0, 25, 50, 75 and 100 wt% rutile that performed in ethanol dehydration reaction at the temperature interval range from 200 to 400 °C are presented in **Figure 26**.

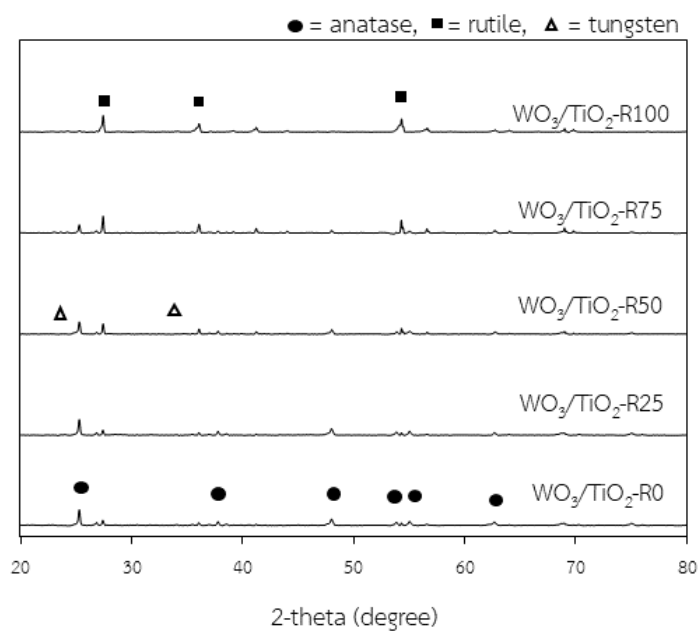


**Figure 26** XRD patterns of the spent catalysts with different phase of  $\text{TiO}_2$

Results show that positions of peaks for all catalysts with different phase are located at the same positions when compare with the results of the catalysts before through the ethanol dehydration reaction. The peaks of anatase phase of titania supports displays at  $25^\circ$  (major),  $37^\circ$ ,  $38^\circ$ ,  $48^\circ$ ,  $54^\circ$ ,  $55^\circ$  and  $75^\circ$ , whereas the peaks of rutile phase of titania support exhibits rutile peaks at  $28^\circ$  (major),  $36^\circ$  and  $54^\circ$ . For  $\text{WO}_3/\text{TiO}_2\text{-R25}$ ,  $\text{WO}_3/\text{TiO}_2\text{-R50}$  and  $\text{WO}_3/\text{TiO}_2\text{-R75}$  catalysts, they display both peaks of anatase and rutile phase with rutile peak intensity increases and anatase peak intensity decreases as % of rutile phase was increased. Because the highest reaction temperature at  $400^\circ\text{C}$  is not exceed the temperature of titania phase changing [18].

## Part II: Stability of $\text{WO}_3/\text{TiO}_2$ catalyst having the highest catalytic activity (from Part I)

After determining the catalytic dehydration reaction of ethanol to diethyl ether and ethylene by  $\text{WO}_3/\text{TiO}_2$  catalysts with different phases of  $\text{TiO}_2$ . It was found that  $\text{WO}_3/\text{TiO}_2$ -R50 catalyst gave the highest diethyl ether yield of 9.0% at  $300^\circ\text{C}$  and ethylene yield of 79.6% at  $350^\circ\text{C}$ . Thus,  $\text{WO}_3/\text{TiO}_2$ -R50 catalyst was selected to study the stability of the catalyst on ethanol dehydration reaction with time on stream in this part.

### 4.2.1 Reaction test

$\text{WO}_3/\text{TiO}_2$ -R50 catalyst was performed in the fixed-bed microreactor on the catalytic dehydration reaction of ethanol to DEE with time on stream at  $300^\circ\text{C}$  for 10 h. The catalytic activities (ethanol conversion, DEE selectivity and DEE yield) are displayed in **Figure 27**.

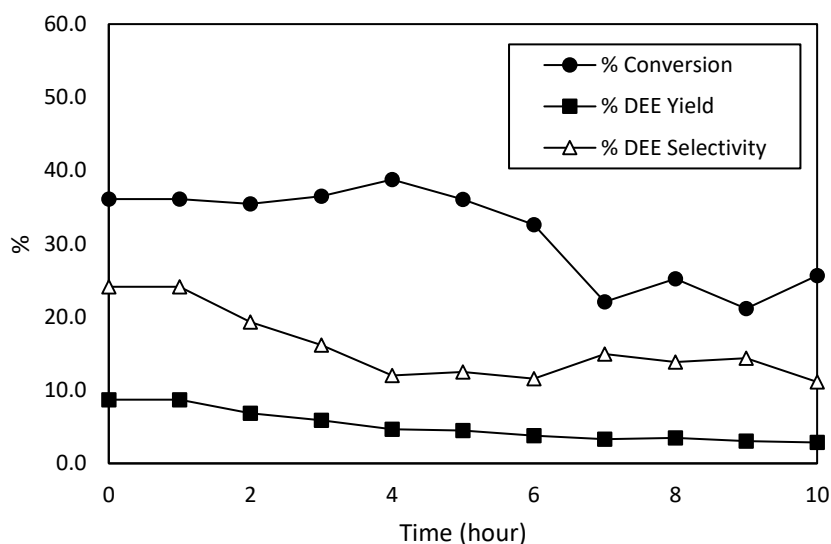


**Figure 27** Activities on the ethanol dehydration at  $300^\circ\text{C}$

It was found that ethanol conversion is relatively stable since the reaction began (36.1%) until the 5<sup>th</sup> hour (36.0%), then the conversion decreases rapidly in the 5-7 hours (36.0% to 22.1%) and is quite stable from the 7<sup>th</sup> hour to the end of the

reaction at the 10<sup>th</sup> hour (25.7%). The DEE selectivity at the beginning of the reaction was 24.1% and decreased rapidly from the 2<sup>nd</sup> hour (19.3%) onwards and is quite stable from the 4<sup>th</sup> hour to the end of the reaction at the 10<sup>th</sup> hour (11.1%). Due to DEE selectivity begins to decrease from the 2<sup>nd</sup> hour onwards, it causes to the DEE yield from the beginning of the reaction at 8.7% gradually decreases to 2.9% in the 10<sup>th</sup> hour.

**Table 9** Ethanol conversion, product selectivity and product yield for the ethanol dehydration reaction at 300 °C

Time (hour)	% Conversion	% Product Selectivity			% Product Yield		
		Ethylene	CH <sub>3</sub> CHO	DEE	Ethylene	CH <sub>3</sub> CHO	DEE
0	36.1	71.8	4.0	24.1	25.9	1.5	8.7
1	36.1	71.8	4.0	24.1	25.9	1.5	8.7
2	35.5	71.1	9.5	19.3	25.2	3.4	6.9
3	36.5	71.8	12.0	16.1	26.2	4.4	5.9
4	38.8	72.6	15.4	12.0	28.1	6.0	4.7
5	36.0	71.6	15.9	12.5	25.8	5.7	4.5
6	32.6	66.7	21.7	11.6	21.7	7.1	3.8
7	22.1	69.0	16.0	14.9	15.2	3.5	3.3
8	25.2	67.2	18.9	13.8	16.9	4.8	3.5
9	21.1	66.2	19.5	14.4	14.0	4.1	3.0
10	25.7	60.8	28.1	11.1	15.6	7.2	2.9

The summary of catalytic activities is presented in **Table 9**. According to the results of this study, it can be concluded that WO<sub>3</sub>/TiO<sub>2</sub>-R50 catalyst was not stable to the ethanol dehydration reaction to DEE.

The catalytic dehydration reaction of ethanol to ethylene with time on stream at 350 °C 10 h was performed by using  $\text{WO}_3/\text{TiO}_2\text{-R50}$  catalysts in the fixed-bed microreactor. The catalytic activities (ethanol conversion, DEE selectivity and DEE yield) are presented in **Figure 28**.

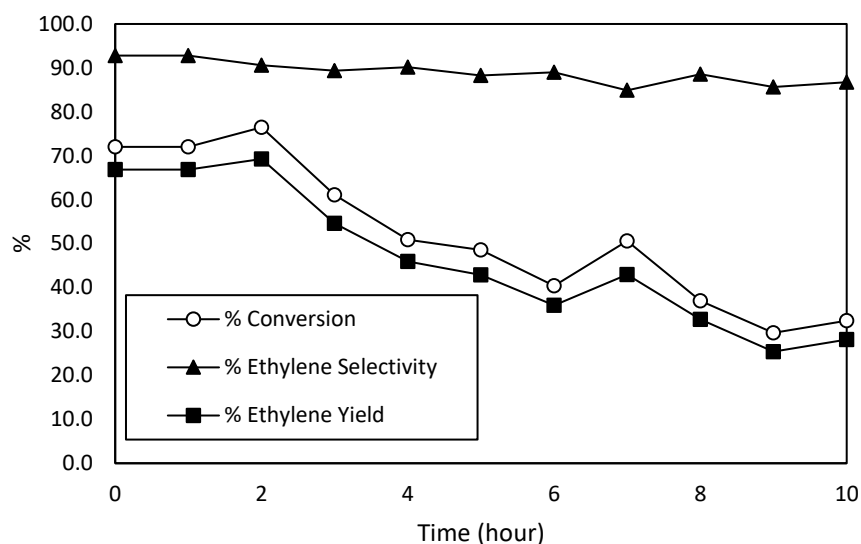


**Figure 28** Activities on the ethanol dehydration at 350 °C

It was found that ethanol conversion is quite stable since the reaction began (72.0%) until the 2<sup>nd</sup> hour (76.5.0%), then the conversion gradually decreases to the end of the reaction at the 10<sup>th</sup> hour (32.4%). The ethylene selectivity slightly decreased over 10 hours of reaction period, with the selectivity of 92.8% at the beginning of the reaction and final selectivity of 86.8% at the end of the reaction. Due to ethanol conversion begins to decrease after the 2<sup>nd</sup> hour onwards, it causes to the ethylene yield from the beginning of the reaction at 66.9%, that is quite stable until the 2<sup>nd</sup> hour at 69.3%, then gradually decreases to 28.1% in the 10<sup>th</sup> hour.

**Table 10** Ethanol conversion, product selectivity and product yield for the ethanol dehydration reaction at 350 °C

Time (hour)	% Conversion	% Product Selectivity			% Product Yield		
		Ethylene	CH <sub>3</sub> CHO	DEE	Ethylene	CH <sub>3</sub> CHO	DEE
0	72.0	92.8	5.3	1.9	66.9	3.8	1.4
1	72.0	92.8	5.3	1.9	66.9	3.8	1.4
2	76.5	90.6	6.9	2.5	69.3	5.3	1.9
3	61.1	89.4	7.9	2.7	54.6	4.8	1.6
4	50.9	90.2	6.5	3.4	45.9	3.3	1.7
5	48.6	88.3	8.3	3.5	42.9	4.0	1.7
6	40.4	89.0	9.8	1.2	35.9	3.9	0.5
7	50.6	84.9	12.0	3.1	43.0	6.1	1.6
8	37.0	88.6	10.3	1.1	32.7	3.8	0.4
9	29.7	85.6	14.4	0.0	25.4	4.3	0.0
10	32.4	86.8	12.3	1.0	28.1	4.0	0.3

The summary of catalytic activities is presented in **Table 10**. According to the results of this study, it can be found that WO<sub>3</sub>/TiO<sub>2</sub>-R50 catalyst is stable for the ethanol dehydration reaction to ethylene at 2 hours.

#### 4.2.2 X-ray diffraction (XRD) for spent catalysts

XRD patterns of  $\text{WO}_3/\text{TiO}_2\text{-R50}$  catalysts after performed ethanol dehydration reaction at 300 °C and 350 °C with time on stream were determined to compare with the spent  $\text{WO}_3/\text{TiO}_2\text{-R50}$  catalyst of ethanol dehydration reaction with temperature program in Part I that is presented in **Figure 29**.

The results display peaks of anatase and rutile phase of titania at the same positions for all samples. Therefore, it can be concluded that the reaction time does not cause the phase change of titania. However, the spent catalyst that was performed the ethanol dehydration with time on steam gave lower intensity of peaks than the fresh catalysts. It indicates that the crystallite size has changed. However, XRD pattern cannot be observed for the tungsten species due to its highly dispersed forms. The crystallite size that was calculated by using Scherrer equation is shown in **Table 11**. It was found that crystallite size of spent catalysts for the reaction at 300 and 350 °C (42.7 and 42.0 nm) is smaller than fresh catalysts (52.0 nm). Thus, no sintering was occurred at the reaction condition.

**Table 11** Average crystalize size of the  $\text{WO}_3/\text{TiO}_2\text{-R50}$  catalysts

Sample	2-theta	$\beta$ (rad)	$d_c$ (nm)
Fresh catalysts	25.3	0.0027	52.0
Spent catalysts for the reaction at 300 °C	25.3	0.0033	42.7
Spent catalysts for the reaction at 350 °C	25.3	0.0034	42.0

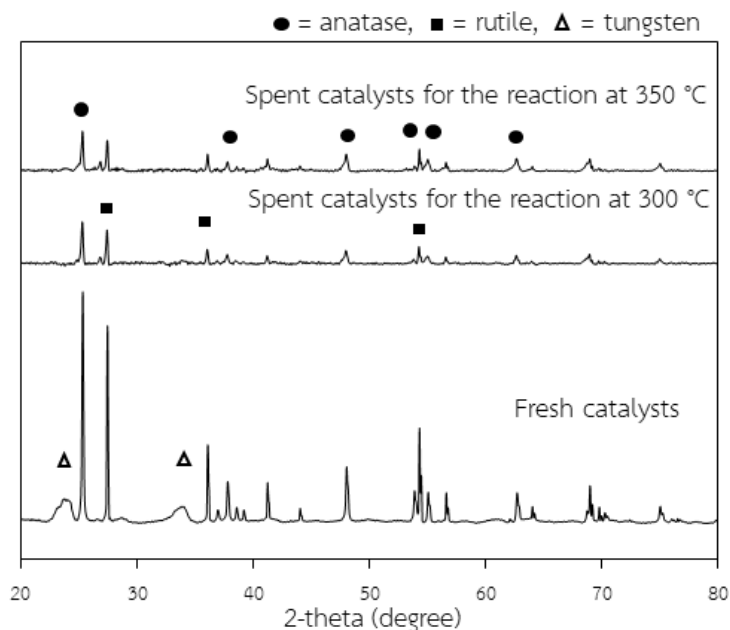
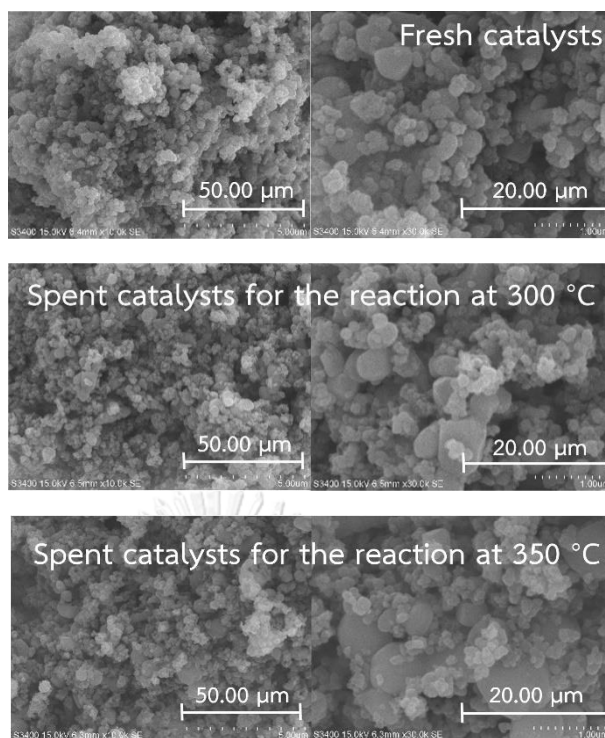


Figure 29 XRD patterns of the spent  $\text{WO}_3/\text{TiO}_2\text{-R50}$  catalysts

#### 4.2.3 Scanning electron microscope (SEM) and energy Dispersive X-ray spectroscopy (EDX) for spent catalysts

SEM shows morphology of  $\text{WO}_3/\text{TiO}_2\text{-R50}$  to compare between fresh catalysts and spent catalysts after being used in ethanol dehydration at 300 °C and 350 °C as shown in **Figure 30**. It was found that the particle size of spent catalysts is slightly larger compared to fresh catalysts. This is because, when the catalyst undergoes a long catalytic reaction, it will result in the sintering of the catalyst and the particle size is larger. However, when compared SEM and XRD techniques as mentioned above, it can be concluded that no sintering was occurred.





**Figure 30** SEM micrographs of  $\text{WO}_3/\text{TiO}_2\text{-R50}$  catalysts

**Figures 31** and **32** present the histogram graph used to display the distribution of the particle size in width and length respectively that were calculated to find the average particle size in width and length according to **Tables 12** and **13**.

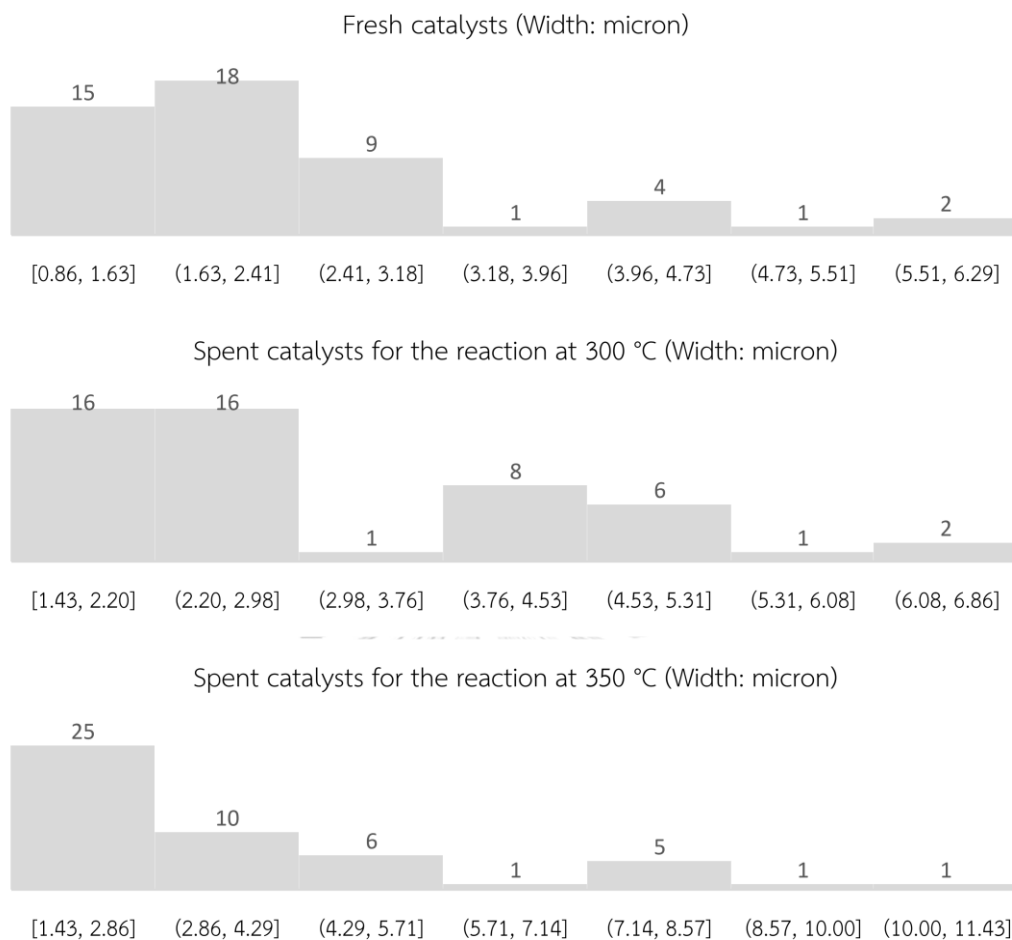
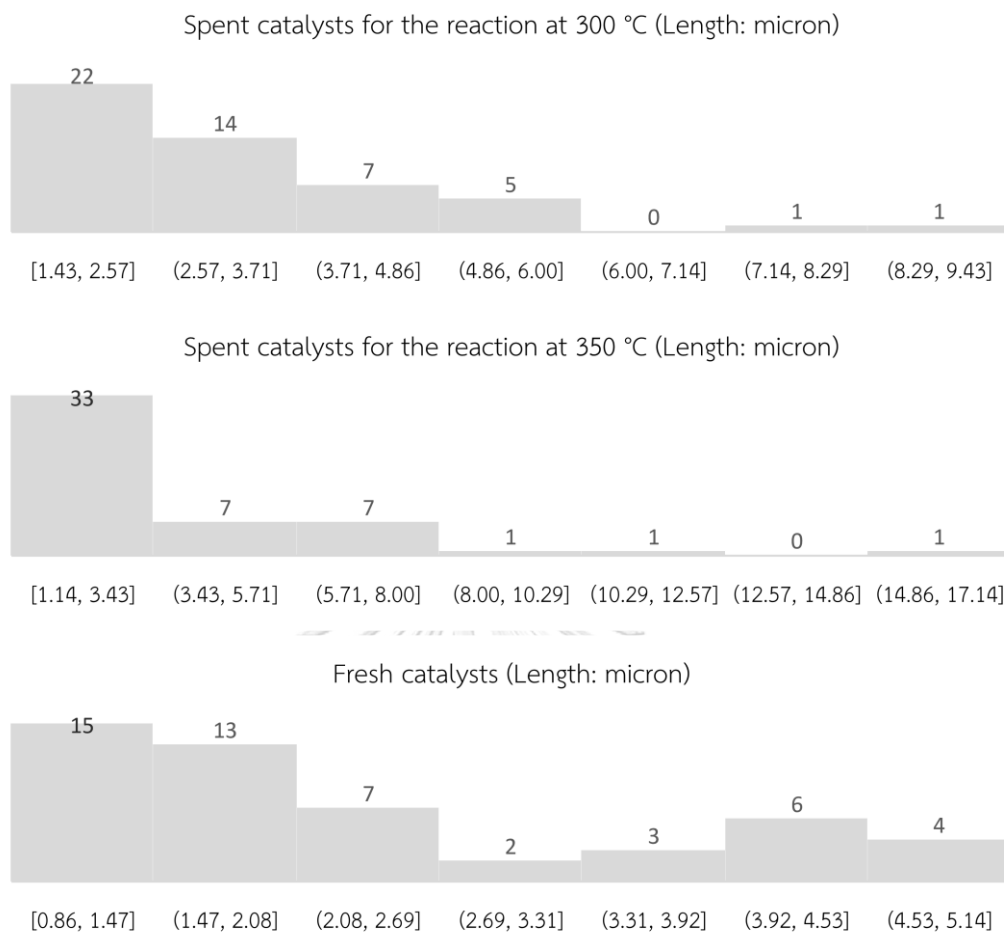


Figure 31 Histogram graph on width of particle sizes of all catalysts



**Figure 32** Histogram graph on length of particle sizes of all catalysts

The results show that the average width of particle size of spent catalysts after performed in the reaction at 300 °C and 350 °C (3.06 and 3.82 micron) is slightly larger than fresh catalysts (2.34 micron) and the average length of particle size of spent catalysts after performed in the reaction at 300 °C and 350 °C (3.13 and 3.92 micron) are slightly larger than fresh catalysts (2.43 micron).

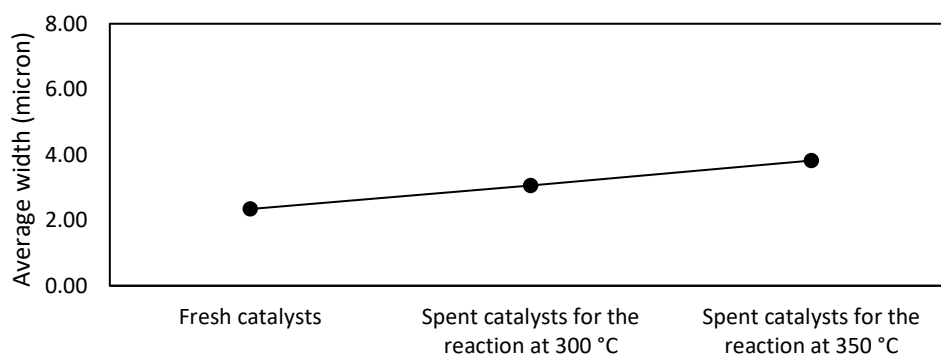
**Table 12** The average width of particle sizes of WO<sub>3</sub>/TiO<sub>2</sub>-R50 catalysts

Catalysts	Width (micron)			
	Min	Max	Mean	S.D.
Fresh catalysts	0.857	6.286	2.34	1.21
Spent catalysts for the reaction at 300 °C	1.429	6.857	3.06	1.37
Spent catalysts for the reaction at 350 °C	1.429	11.429	3.82	2.35

**Table 13** The average length of particle sizes of WO<sub>3</sub>/TiO<sub>2</sub>-R50 catalysts

Catalyst	Length (micron)			
	Min	Max	Mean	S.D.
Fresh catalysts	0.857	5.143	2.43	1.24
Spent catalysts for the reaction at 300 °C	1.429	9.429	3.13	1.69
Spent catalysts for the reaction at 350 °C	1.143	17.143	3.92	2.98

The average particle sizes of all catalysts are displayed in **Figures 33 and 34**. It can be concluded that high temperature of the reaction (350 °C) giving the particle sizes is slightly larger than those at low temperature of the reaction (300 °C) and slightly larger than fresh catalysts.

**Figure 33** The average width particle size of all catalysts

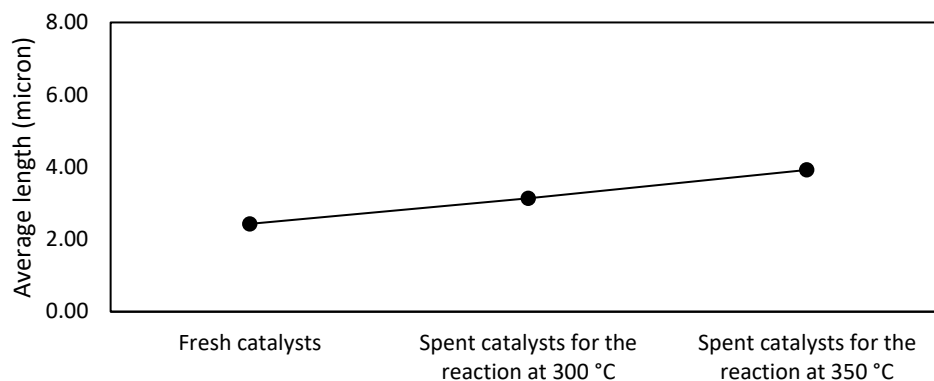


**Figure 34** The average length particle size of all catalysts

Coke formation of  $\text{WO}_3/\text{TiO}_2\text{-R50}$  catalyst after being used in the ethanol dehydration reaction at temperature 300 and 350 °C was determined by measuring %carbon with EDX analysis and the results are displayed in the **Table 14**

**Table 14** The amount of %carbon in the spent catalysts with operating temperature

Catalysts	%Carbon	Operating Temperature (°C)
$\text{WO}_3/\text{TiO}_2\text{-R50}$	1.46	300
$\text{WO}_3/\text{TiO}_2\text{-R50}$	1.63	350

From the table, it was found that  $\text{WO}_3/\text{TiO}_2\text{-R50}$  with operating temperature at 350 °C gives slightly higher %carbon of 1.63% than that from  $\text{WO}_3/\text{TiO}_2\text{-R50}$  with operating temperature at 300 °C having %carbon of 1.46%. This is because coke formation prefers to occur in high temperature

Coke formation in  $\text{WO}_3/\text{TiO}_3\text{-R50}$  catalyst is the major cause of deactivation leading to carbon deposition on the active sites. The results of lower active sites led to lower catalytic activities of ethanol dehydration reaction.

#### 4.2.4 Catalysts appearance

The appearance of  $\text{WO}_3/\text{TiO}_2$  - R50 catalysts was presented to observe the color change of before and after ethanol dehydration reaction at 300 °C and 350 °C.

The image of the catalysts is presented in **Figure 35**.

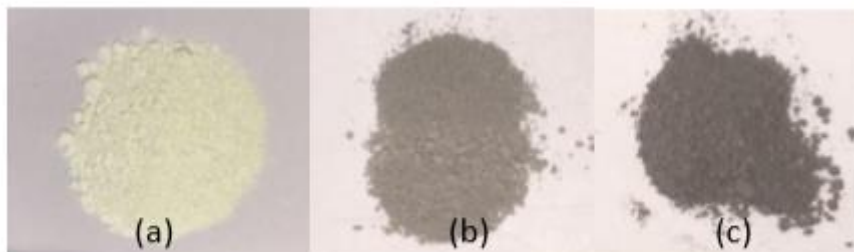


**Figure 35** The appearance of  $\text{WO}_3/\text{TiO}_2$  - R50 catalyst (a) fresh catalysts (b) spent catalysts for ethanol dehydration at 300 °C (c) spent catalysts for ethanol dehydration at 350 °C

The coke formation was observed by the color change from yellow color to grey color after all catalysts were being used in ethanol dehydration reaction with time on stream for 10 h. Also, when comparing the spent catalysts for ethanol dehydration reaction at 300 and 350 °C, it was found that the appearance of spent catalysts for ethanol dehydration reaction at temperature of 350 °C, is darker than the ethanol dehydration reaction at temperature of 300 °C. The results are consistent with the carbon percentage as determined by EDX analysis.

Part III: The comparison of catalysts for diethyl ether and ethylene synthesis and their catalytic activity

**Table 15** Comparison of catalysts for DEE and ethylene synthesis and their catalytic activity

Catalyst	Total acidity ( $\mu\text{mol/g cat}$ )	Weak to strong acid site ratio	Reaction temperature ( $^{\circ}\text{C}$ )	Ethanol conversion (%)	Ethylene yield (%)	DEE yield (%)	Ref.
$\text{WO}_3/\text{TiO}_2$ - R0	1988.5	0.85	200-400	0-52.4	0-49.2	0-7.1	This study
$\text{WO}_3/\text{TiO}_2$ - R25	1002.2	0.94	200-400	0-61.2	0-53.6	0-8.1	This study
$\text{WO}_3/\text{TiO}_2$ - R50	1281.5	0.97	200-400	0-84.0	0-79.6	0-9.0	This study
$\text{WO}_3/\text{TiO}_2$ - R75	800.2	0.79	200-400	0-50.6	0-43.9	0-6.9	This study
$\text{WO}_3/\text{TiO}_2$ - R100	615.2	0.55	200-400	0-55.2	0-50.6	0-7.1	This study
G-Al-B	658	2.4	200-400	14-85	0-78.0	7.2-30.7	[25]
C-Al-B	776	1.9	200-400	16-85	0-75.9	9.9-27.0	[25]
M-Al-B	635	3.3	200-400	15-100	0-92.3	7.3-48.3	[25]
HBZ	1517	-	250	66	42.9	35	[26]
Ru-HBZ	1320	-	250	73	53.655	47	[26]
Pt-HBZ	1442	-	250	70	48.86	45	[26]
HZSM-5	974	2.2	200	81.3-100	11.4-96.4	0-12	[27]
2%PHZSM-5	705	3.0	300	100	94.5	0	[27]

**Table 15** presents the summary of the catalytic activity for ethanol dehydration reaction to diethyl ether and ethylene over various catalysts. It is displayed that  $\text{WO}_3/\text{TiO}_2$  catalysts in this study are comparable to other catalysts.

## CHAPTER 5

### CONCLUSIONS AND RECOMMENDATIONS

In this study, the results of  $WO_3/TiO_2$  catalysts with different phases of  $TiO_2$  (anatase, rutile and mixed phases) including 0, 25, 50, 75 and 100 wt% of rutile were investigated. The stability of catalyst having the highest catalytic properties was also determined to evaluate the characteristics and catalytic performance via ethanol dehydration reaction. Therefore, the research conclusions and recommendations are explained in **sections 5.1** and **5.2**, respectively.

#### 5.1 Conclusions

1. The portion of phase composition of  $TiO_2$  support causes changes in catalytic properties and the catalytic behavior of  $WO_3/TiO_2$  catalyst in the ethanol dehydration.
2. Particle size of catalyst with high portion of rutile phase as support is larger than the catalysts which contain low portion of rutile phase as support. Corresponding to low surface area of catalyst with high portion of rutile phase as support. Furthermore, the presence of rutile phase in  $TiO_2$  support significantly affects the decreased surface area.
3. The highest activity on the ethanol dehydration to DEE and ethylene obtained from the  $WO_3/TiO_2$ -R50 catalyst can be attributed to the highest weak to strong acid site ratio.
4.  $WO_3/TiO_2$ -R50 catalyst gave the highest ethylene yield (79.6%) at 350°C and DEE yield (9.0%) at 300 °C for ethanol dehydration.
5. The catalytic ethanol dehydration reaction in range of temperature at 200-400 °C, does not cause the  $TiO_2$  phase change.
6. Catalyst with rutile phase as support, loses acidity more easily than using anatase phase as supports, but it is better resistant for coke formation.



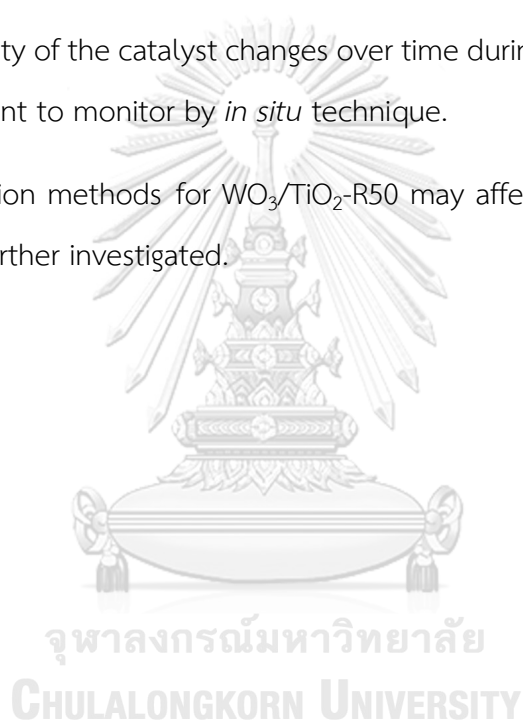
7.  $\text{WO}_3/\text{TiO}_2$ -R50 catalyst is stable for the ethanol dehydration reaction to ethylene at 2 hours, but it is not stable for DEE production.

8. The long ethanol dehydration reaction time causes coke formation in catalysts. It is a factor to decrease active site on surface area due to surface coverage by coke, leading to lower catalytic activity.

## 5.2 Recommendations

1. The acidity of the catalyst changes over time during the ethanol dehydration reaction is important to monitor by *in situ* technique.

2. Preparation methods for  $\text{WO}_3/\text{TiO}_2$ -R50 may affect the catalytic properties. So, it should be further investigated.



## REFERENCES

1. Tunpaiboon, N., *Thailand Industry Outlook 2017-19 Ethanol*. Krungsri Research, 2017.
2. พ.ร.บ.กองทุนน้ำมันฯ ประกาศในราชกิจจานุเบกษา เตรียมยกเลิกอุดหนุนเชื้อเพลิงชีวภาพใน3ปี. 2019; Available from: <http://www.energynewscenter.com/พ-ร-บ-กองทุนน้ำมัน-ประกาศ/>.
3. Kamsuwan, T. and B. Jongsomjit, *Characterization of Different Si- and Al-based Catalysts with Pd Modification and Their Use for Catalytic Dehydration of Ethanol*. *J Oleo Sci*, 2018. **67**(8): p. 1005-1014.
4. Sun, J. and Y. Wang, *Recent Advances in Catalytic Conversion of Ethanol to Chemicals*. *ACS Catalysis*, 2014. **4**(4): p. 1078-1090.
5. *Department of Alternative Energy Development and Efficiency, Alternative Energy Development Plan: AEDP2015*. 2015.
6. Rawat, J., P. Rao, and V. Nettem, *Effect of Ethanol-Gasoline Blends on Corrosion Rate in the Presence of Different Materials of Construction used for Transportation, Storage and Fuel Tanks*. 2019.
7. *Ethanol as Fuel for Road Transportation*. NSTDA, 2010.
8. จากรถยนต์น้ำมัน สู่ ‘รถยนต์ไฟฟ้า’ เป็นไปได้แค่ไหนกับประเทศไทย. 2019; Available from: <https://themomentum.co/electric-vehicle-thailand-2019/>.
9. รายงานสถิติ. Available from: [http://www.customs.go.th/statistic\\_report.php?show\\_search=1](http://www.customs.go.th/statistic_report.php?show_search=1).
10. Widayat, A. Roesyadi, and M. Rachimoellah, *Diethyl Ether Production Process with Various Catalyst Type*. *Internat. J. of Sci. and Eng.*, 2013. **4**(1): p. 6-10.
11. Soh, J.C., et al., *Catalytic ethylene production from ethanol dehydration over non-modified and phosphoric acid modified Zeolite H-Y (80) catalysts*. *Fuel Processing Technology*, 2017. **158**: p. 85-95.
12. Zhang, M. and Y. Yu, *Dehydration of Ethanol to Ethylene*. *Industrial & Engineering Chemistry Research*, 2013. **52**(28): p. 9505-9514.

13. Phung, T.K., et al., *Dehydration of ethanol over zeolites, silica alumina and alumina: Lewis acidity, Brønsted acidity and confinement effects*. Applied Catalysis A: General, 2015. **493**: p. 77-89.
14. Phung, T.K., L. Proietti Hernández, and G. Busca, *Conversion of ethanol over transition metal oxide catalysts: Effect of tungsta addition on catalytic behaviour of titania and zirconia*. Applied Catalysis A: General, 2015. **489**: p. 180-187.
15. Jongsomjit, B., T. Wongsalee, and P. Prasertthdam, *Characteristics and catalytic properties of Co/TiO for various rutile:anatase ratios*. Catalysis Communications, 2005. **6**(11): p. 705-710.
16. Gavahian, M., et al., *Emerging techniques in bioethanol production: from distillation to waste valorization*. Green Chemistry, 2019. **21**(6): p. 1171-1185.
17. Tresatayawed, A., P. Glinrun, and B. Jongsomjit, *Ethanol Dehydration over WO<sub>3</sub>/TiO<sub>2</sub> Catalysts Using Titania Derived from Sol-Gel and Solvothermal Methods*. International Journal of Chemical Engineering, 2019. **2019**: p. 1-11.
18. Al-Eqaby, H.H.H., *Fabrication of TiO<sub>2</sub> Nanotubes Using Electrochemical Anodization Republic of Iraq Fabrication of TiO<sub>2</sub> Nanotubes Using Electrochemical Anodization*. 2012.
19. Sritaweewat, T. and A. Chaikhun, *Synthesis of Cu/SiO<sub>2</sub>-Al<sub>2</sub>O<sub>3</sub> For Catalytic Reduction of Nitric Oxide*. 2012.
20. Wagner, T., et al., *Mesoporous materials as gas sensors*. Chem Soc Rev, 2013. **42**(9): p. 4036-53.
21. Phung, T.K. and G. Busca, *Ethanol dehydration on silica-aluminas: Active sites and ethylene/diethyl ether selectivities*. Catalysis Communications, 2015. **68**: p. 110-115.
22. Jongsomjit, B., T. Wongsalee, and P. Prasertthdam, *Study of cobalt dispersion on titania consisting various rutile:anatase ratios*. Materials Chemistry and Physics, 2005. **92**(2-3): p. 572-577.
23. Raj, K.J.A. and B. Viswanathan, *Effect of surface area, pore volume and particle size of P25 titania on the phase transformation of anatase to rutile*. Indian Journal of Chemistry, 2009. **48A**: p. 1378-1382.

24. Kerdnoi, P., et al., *Catalytic Dehydration of Ethanol over WTiO<sub>2</sub> Catalysts Having Different Phases of Titania*. TIChE, 2017.
25. Chaichana, E., et al., *Catalytic dehydration of ethanol to ethylene and diethyl ether over alumina catalysts containing different phases with boron modification*. Journal of Porous Materials, 2018. **26**(2): p. 599-610.
26. Kamsuwan, T., P. Prasertdam, and B. Jongsomjit, *Diethyl Ether Production during Catalytic Dehydration of Ethanol over Ru- and Pt- modified H-beta Zeolite Catalysts*. J Oleo Sci, 2017. **66**(2): p. 199-207.
27. Zhan, N., et al., *Lanthanum-phosphorous modified HZSM-5 catalysts in dehydration of ethanol to ethylene: A comparative analysis*. Catalysis Communications, 2010. **11**(7): p. 633-637.





APPENDIX

จุฬาลงกรณ์มหาวิทยาลัย  
**CHULALONGKORN UNIVERSITY**

## APPENDIX A

## CALCULATION FOR CATALYST PREPARATION

Calculation for preparation of 13.5 wt% of tungsten loading on different phase of TiO<sub>2</sub> supports

**Catalyst:** Tungsten (VI) chloride (WCl<sub>6</sub>)

Molecular weight = 396.61 g/mol

Tungsten (W) weight = 183.84 × 1 = 183.84 g/mol

**Support:** Titania (TiO<sub>2</sub>) supports: anatase and rutile

Basis 1 g of catalyst;

13.5 wt% of tungsten (W) = 0.135 g

There is 183.84 g of W in 396.61 g of tungsten (VI) chloride

Thus, there is 0.135 g of W in  $0.135 \times 396.61 / 183.84$

= 0.291 g of tungsten (VI) chloride

TiO<sub>2</sub>-RXX support = 1.00 - 0.135 = 0.865 g

(1) TiO<sub>2</sub>-R0 support = 0 × 0.865 g = 0 g of rutile phase

Thus, there is anatase phase in TiO<sub>2</sub> = 0.865 - 0 g = 0.865 g

(2) TiO<sub>2</sub>-R25 support = 0.25 × 0.865 g = 0.216 g of rutile phase

Thus, there is anatase phase in TiO<sub>2</sub> = 0.865 - 0.216 g = 0.649 g

(3) TiO<sub>2</sub>-R50 support = 0.50 × 0.865 g = 0.432 g of rutile phase

Thus, there is anatase phase in TiO<sub>2</sub> = 0.865 - 0.432 g = 0.433 g

(4) TiO<sub>2</sub>-R75 support = 0.75 × 0.865 g = 0.649 g of rutile phase

Thus, there is anatase phase in TiO<sub>2</sub> = 0.865 - 0.649 g = 0.216 g

(5)  $\text{TiO}_2\text{-R100 support} = 1.00 \times 0.865 \text{ g} = 0.865 \text{ g}$  of rutile phase

Thus, there has not anatase phase in  $\text{TiO}_2$

Then, tungsten (VI) chloride ( $\text{WCl}_6$ ) was dissolved in deionized water and impregnated onto  $\text{TiO}_2$  supports with physical mixing to obtain non-calcined  $13.5\text{W}/\text{TiO}_2\text{-R0}$ ,  $13.5\text{W}/\text{TiO}_2\text{-R25}$ ,  $13.5\text{W}/\text{TiO}_2\text{-R50}$ ,  $13.5\text{W}/\text{TiO}_2\text{-R75}$  and  $13.5\text{W}/\text{TiO}_2\text{-R100}$  catalysts, respectively.



**APPENDIX B**  
**CALCULATION FOR ACIDITY**

The acidity of all catalysts is determined from NH<sub>3</sub>-TPD by calculating the area under TCD signal versus temperature.

$$\text{Acidity of catalysts} = \frac{\text{Mol of desorbed NH}_3}{\text{Weight of dry catalyst}} \quad [\mu\text{mol/g cat}]$$

Where mol of desorbed NH<sub>3</sub> = (area under TCD signal curve) × (30.927 μmol)

weight of dry catalyst = 0.05 g

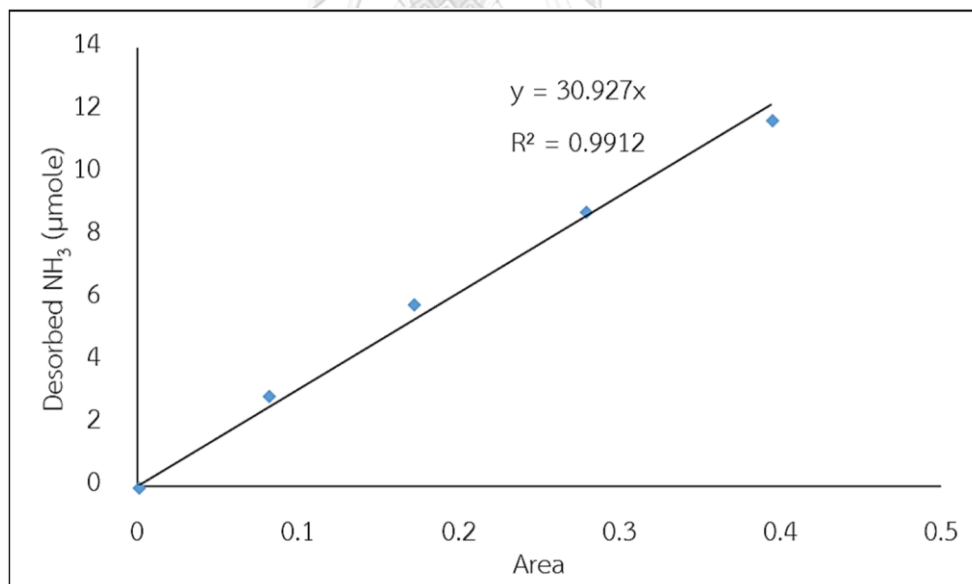


**Figure B.1** The calibration curve of NH<sub>3</sub>-TPD



## APPENDIX C

## CALIBRATION CURVES OF REACTANT AND PRODUCTS

The calibration curves of reactant and products were used to calculate the amount of reactant and products including ethanol, ethylene, acetaldehyde and diethyl ether as showed in **Figure C.1-C.4**.

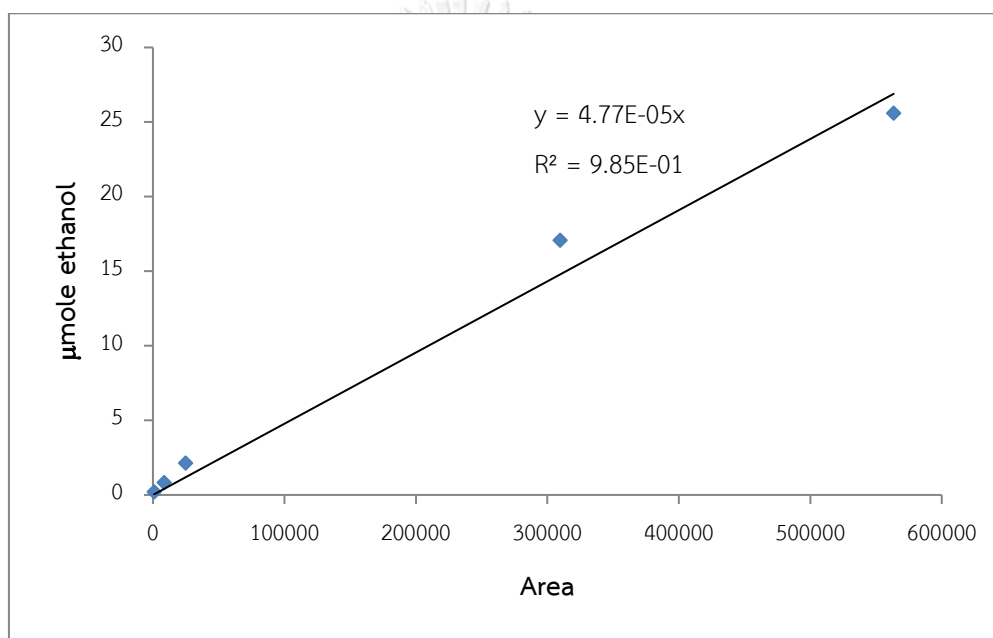


Figure C.1 The calibration curve of ethanol

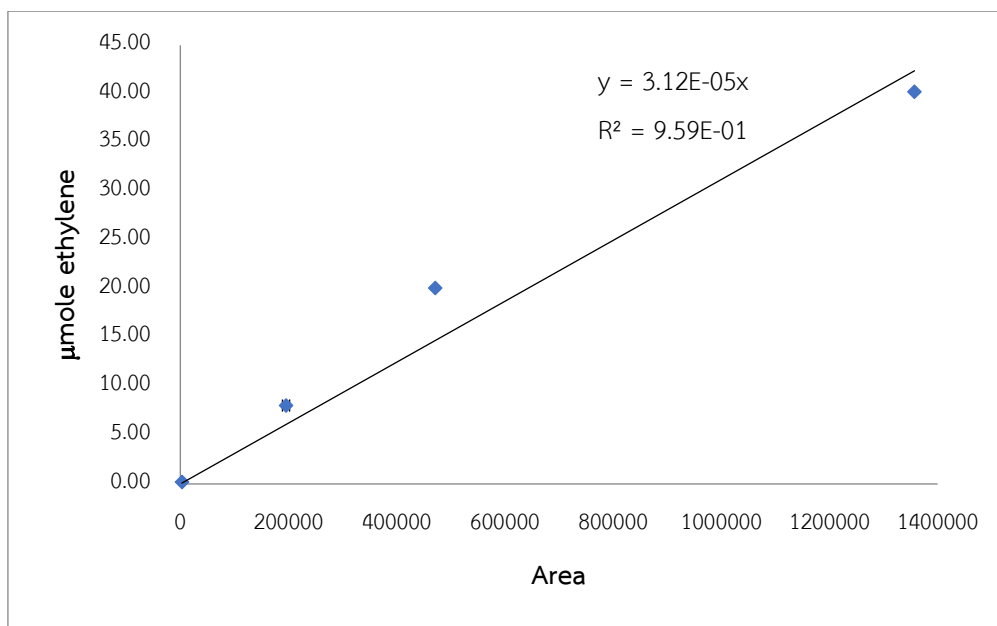


Figure C.2 The calibration curve of ethylene

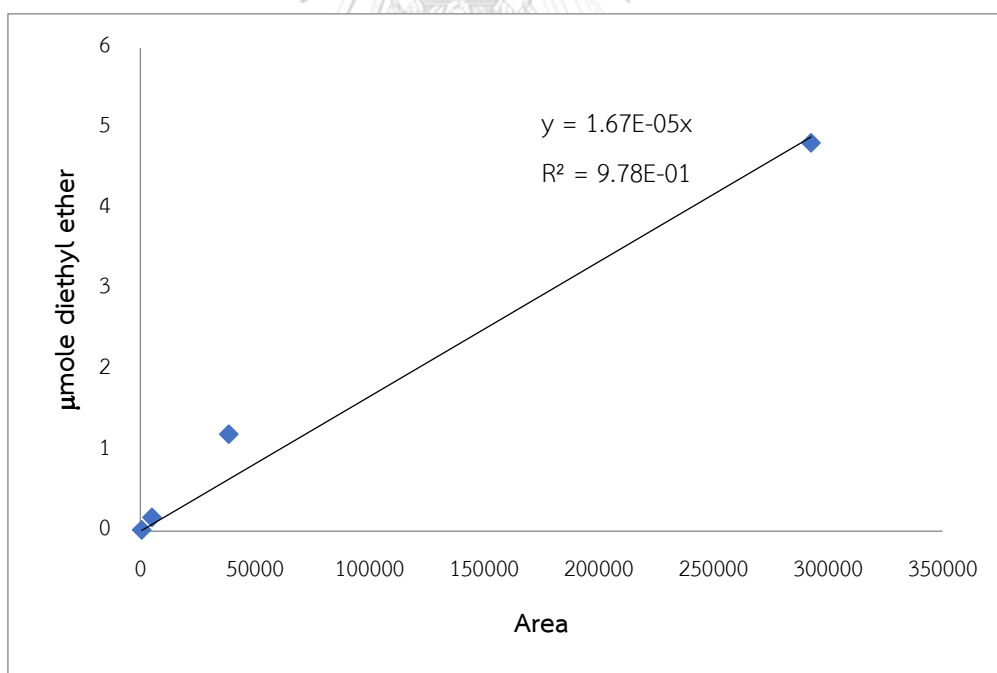


Figure C.3 The calibration curve of diethyl ether

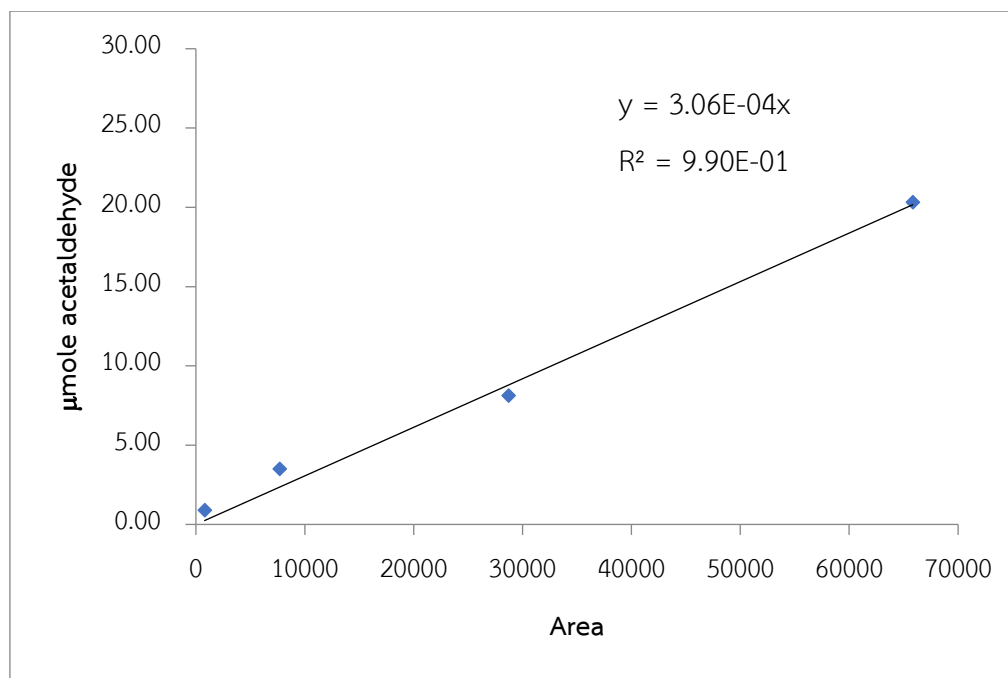


Figure C.4 The calibration curve of acetaldehyde



APPENDIX D  
CHROMATOGRAM

The peak positions of reactant and products showed as below;

**Reactant:** ethanol peak position = 4.6 min

**Products:** ethylene peak position = 4.1 min

acetaldehyde peak position = 4.3 min

diethyl ether peak position = 4.9 min



## APPENDIX E

## CALCULATION FOR CRYSTALLITE SIZE (SCHERRER EQUATION)

The crystallite size of catalysts was calculated by Scherrer Equation as following;

$$d_c = \frac{k \lambda}{\beta \cos \theta} \quad [\text{nm}]$$

Where

$d_c$  is the mean crystallite size (nm)

$k$  is a dimensionless shape factor ( $k = 0.9$ )

$\lambda$  is the X-ray wavelength ( $\lambda = 0.1544$  nm)

$\beta$  is the line broadening at half the maximum intensity (FWHM)

( $\beta = \Delta(2\theta)$ )

$\theta$  is the Bragg angle

APPENDIX F  
LIST OF PUBLICATION

**Proceeding**

Phatthraporn Termvoratham and Bunjerd Jongsomjit, “Effect of Phase Composition in  $\text{TiO}_2$  on  $\text{WO}_3/\text{TiO}_2$  Catalysts toward Catalytic Ethanol Dehydration to Ethylene and Diethyl Ether” Proceeding of the 1<sup>st</sup> Thailand Biorefinery Conference “The Future of Biorefinery for Thailand 4.0”, Suranaree University of Technology, Nakhon Ratchasima, Thailand, July 25-26, 2019.



## VITA

NAME Phatthraporn Termvoratham  
DATE OF BIRTH 17 August 1993  
PLACE OF BIRTH Bangkok, Thailand



จุฬาลงกรณ์มหาวิทยาลัย  
**CHULALONGKORN UNIVERSITY**